Roinn Cumarsáide, Gníomhaithe ar son na hAeráide & Comhshaoil
Department of Communications, Climate Action & Environment

Geological Survey
Suirbhéireacht Gheolaíochta
Ireland | Éireann

Research Programme
- Short Call 2020, Final Report -

Lead Applicant Name	Jennifer Keenahan
Host Organisation name	University College Dublin
Project Title	Developing seabed scour assessment and prediction tools using computational fluid dynamics modelling (DeMo)
Contract Number	2020-SC-001

This report covers the period 1st December 2020 to project end date 31st January 2022

2. **(a) Project information**:

Final project report (*max 2500 words, excluding figures and headings*):

Executive summary (lay abstract, approx. 250 words):

Seabed hydrodynamics and sediment mobility pose significant threats to offshore engineering infrastructure, not least of all renewable energy installations such as turbine monopile foundations. Such infrastructure can introduce seafloor obstacles that perturb the local environment inducing scour that can cause structural instability, or deposition resulting in the burying of infrastructure. Understanding the processes that drive these complex patterns of sediment erosion and deposition over varying timescales is critical to the sustainable development of critical offshore infrastructure. Traditionally assessments for such issues have utilised time-lapse bathymetric surveys and scaled physical testing. The former fails to capture the nuance of these processes between data collection surveys and cannot predict how the seabed will react to an obstacle, whilst the latter is costly and limited in recreating the marine environment. Computational Fluid Dynamics (CFD) modelling however, offers an effective means of investigating the complex interaction between hydrodynamics and manmade objects on the seafloor. Similarly, shipwrecks offer natural laboratories with which to validate models using CFD approaches. In this study, CFD simulations are generated for two high-resolution bathymetric survey datasets at shipwreck sites in the Irish Sea and used in conjunction with repeat survey data in order to understand temporal sediment dynamics and morphological change at a localised level. This approached was assessed for application in future sediment dynamics and scour prediction studies. Modelled outputs for current flow and stress patterns correspond well with known seabed signatures for sediment erosion and deposition from survey data.

(i) Results, scientific/engineering targets reached beyond the state of the art and conclusions

CFD model outputs for flow velocity, flow patterns and bed shear stress were visualised and analysed in ArcMap version 10.7 and Paraview version 5.9.0 for two shipwreck sites: *SS Polwell* and *SS Hare* (Figure 1), which had been mapped under the INFOMAR programme and again in 2019 as part of the CV19027 GIST survey. Analysis was carried out on results from two separate simulations at each site representing the dominant flow directions.

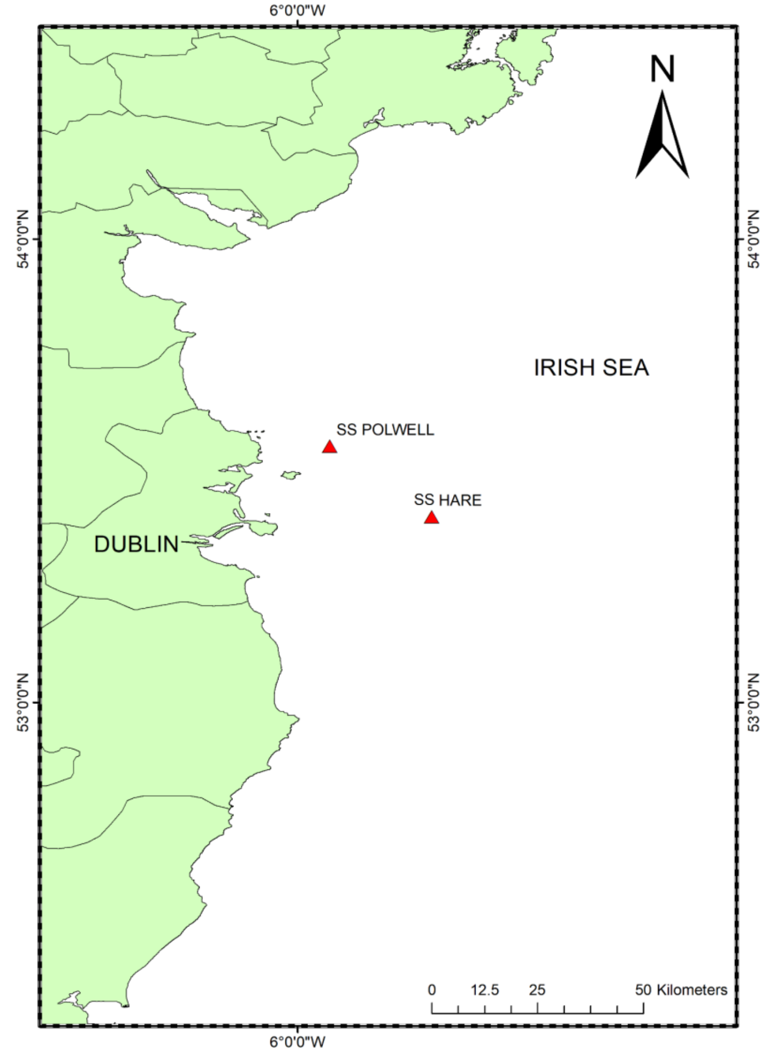

Figure 1 Location of wreck sites modelled as part of this study

Results for Flow Velocity and Patterns

Initially, bed flow velocity values were derived from the cells immediately adjacent to the seabed. Figure 2 shows results for these values as calculated at the *SS Polwell* site. Analysis exhibits a maximum velocity value of 0.26m/s and a minimum value of 0.001m/s for the NW to SE flow and a maximum of 0.25m/s and a minimum of 0.006 for the SE flow. The mean current speed for the NE was 0.09m/s, and 0.08m/s for the SE. Flow rates from the NW were divided and categorized as low velocity (0.001-0.07m/s), medium velocity (0.07-0.12m/s) and high velocity (>0.12m/s), based on the Jenks natural breaks classification of the velocity distribution. The Jenks natural breaks classification method determines the best arrangement of values into different classes by minimizing each class's average deviation from the mean, while maximizing each class's deviation from the means of the other groups (Chen et al., 2013). Flow rates for the SE were categorised as low velocity (0.0006-0.06m/s), medium velocity (0.06-0.11m/s), and high velocity (>0.11m/s).

Flow from the NW displays a large area of high velocity flow, directly in the central wake of the wreck (Figure 1a). This area is surrounded on either side by a low velocity area, wrapping itself around the wreck's bow and stern, producing a typical wake flow. The flow from the bow appears much more pronounced, flowing through the large break in the hull.

Another small area of high velocity flow emerges on the outside of the bow wake, sandwiching the lower velocity flow in between itself and the central wake. As the approach flow makes contact with the wreck on its starboard side it produces two distinct areas of low velocity; at the stern and at the break in the midsection. The areas of high and low velocity are paralleled by a mid-velocity flow on either side. The high velocities in the flow from the SE to NW are concentrated mainly towards the bow of the wreck, pushing through the gap in the bow. The high velocity wake is intersected by a thin stream of low velocity flow and bordered by another to the SW. A large low velocity wake emerges from the stern, separated from the main high velocity wake by a low-mid flow. Again, the approach flow produces areas of low velocity upon reaching the wreck directly, however they span the entirety of the wreck from bow to stern, with a small high velocity area appearing in front of the separated bow section. A medium velocity flow runs either side of the main wake.

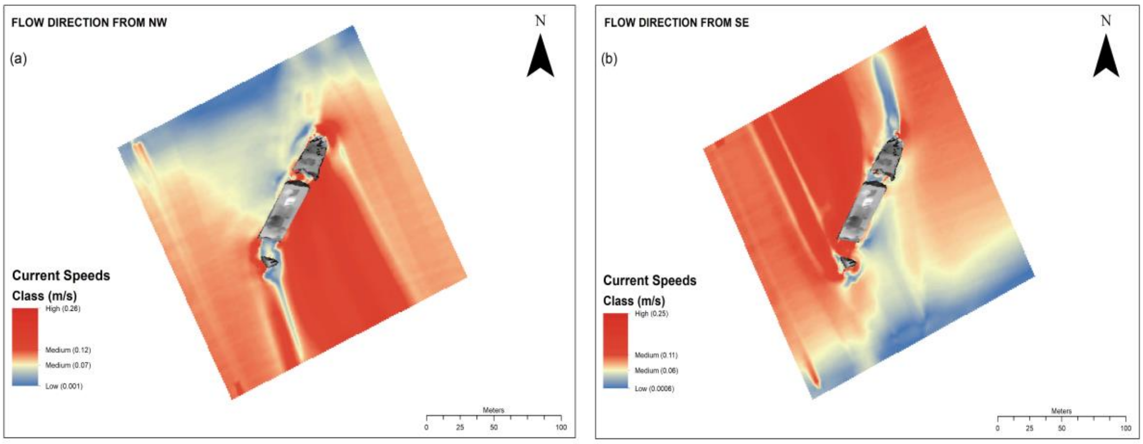

Figure 2. *Maps representing velocities close to the seabed for (a) flow from the NW and (b) flow from the SE*

Streamline models were generated in ParaView for both current directions (Figures 3), showing more complex flow velocity patterns overlaid on bed shear stress values. Flow velocity for both directions ranged from 0.0047m/s to 0.22m/s. Figure 3a shows the flow from the NW to SE. Laminar flow is dominant either side of the bow and stern of the wreck, where shear stress is minimal. As the flow interacts directly with the wreck however, complex patterns emerge in the wake where horizontal flow separation occurs. As water flows around the wreck's stern, it turns inward towards the wreck where two major low velocity vortices form. These vortices occur where the bed shear stress is highest, losing rotation as they continue towards the outflow of the study area. The break towards the ship's stern appears to be a major contributing factor towards the formation of these vortices.

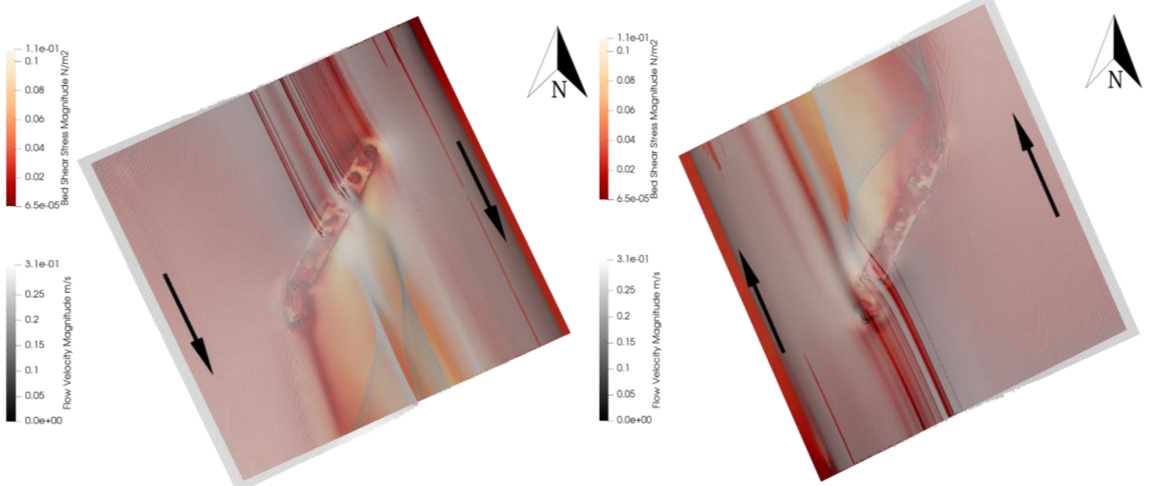

Figure 3. *Streamlines representing flow velocity (a) from NW to SE (b) from SE to NW*

The SE to NW flow shows a similar pattern of vortices where it interacts with the wreck, with steady, laminar flows either side (Figure 3b). Similarly, it shows the formation of two distinct vortices, through the gap in the hull towards the bow of the ship; the first, towards the east is a significantly developed, low velocity vortex stretching all the way to the stern before being contained by the surrounding flow; the second, towards the west, is a far less developed vortex, distinguished from the surrounding flow by its lower velocity and slight rotation. Again, where both vortices occur bed shear stress is at its highest.

<u>Results of Bed Shear Stress</u>

In sediment mobility studies, current speeds are converted to bed shear stress to assess the force acting on a particular sediment type (e.g. Whitehouse, 1998). Figure 4 shows bed shear stress overlaid with areas exhibiting erosional and depositional signatures defined from survey data by Majcher et al. (2021). The flow originating from the NW displays a maximum value of 0.091Pa and a minimum of 0.00008Pa, with a mean of 0.03Pa (Figure 4a). Flow from the SE displays a maximum value of 0.085Pa and a minimum of 0.00008Pa, with a mean of 0.026Pa (Figure 4b). Both flow directions were also characterized separately as having areas of high, medium, and low shear stress based on natural breaks in the data distribution. Flow rates for the NW were categorised as low shear stress (0.00008-0.02Pa), medium shear stress (0.02-0.04Pa), and high shear stress (>0.04Pa). Flow rates for the SE were categorised as low shear stress (0.00008-0.02Pa), medium shear stress (0.02-0.05Pa), and high shear stress (>0.05Pa). Flow from the NW displays a large area of high shear stress in the centre of the wreck's wake, surrounded on either side by areas of low stress. Another, thin area of high stress wraps around the highly defined low stress emerging from the wake of the wreck's bow. There is a small area of high stress in the midship break and a prominent one at the point of the wreck's stern. A large area of low stress is present in the approach flow, making contact with the full length of the wreck. Areas of medium stress are present on either side of the wake. Flow from the SE displays a large area of high stress in the wreck's wake, skewed towards the bow. Two thin lines of low stress emerge on the SW side of the high stress; one intersecting an area of medium-high stress; the other bordering it. A large, well-defined area of low stress emerges from the stern wake, with a very small area of high stress at the point of the stern and a slightly larger one in the gap between the bow and the main section. As with the NE flow, the approach flow contains a large, low stress area that makes contact along the length of the wreck.

The seabed signature patterns of erosional and depositional areas suggest a symmetry, with significant erosional areas adjacent to the wreck on the west side and the east side. A separate large area of deposition occurs to the SE, with a thin signature of low deposition slightly north. Neither of these areas show a symmetrical comparison to the NW. The areas of erosion and deposition represented by the previous survey data compare well with the areas of high and low shear stress generated from the model outputs. In the wreck's wake the boundaries outlining erosional effects follow the model predictions closely, with high shear stress in the centre. The areas outside this high stress area, where velocity and shear stress drop to low values, are outlined by areas of deposition from the survey data. The *SS Polwell* itself is located in a signature indicating an area of deposition, with the model outputs showing low shear stress in the vicinity of the wreck body.

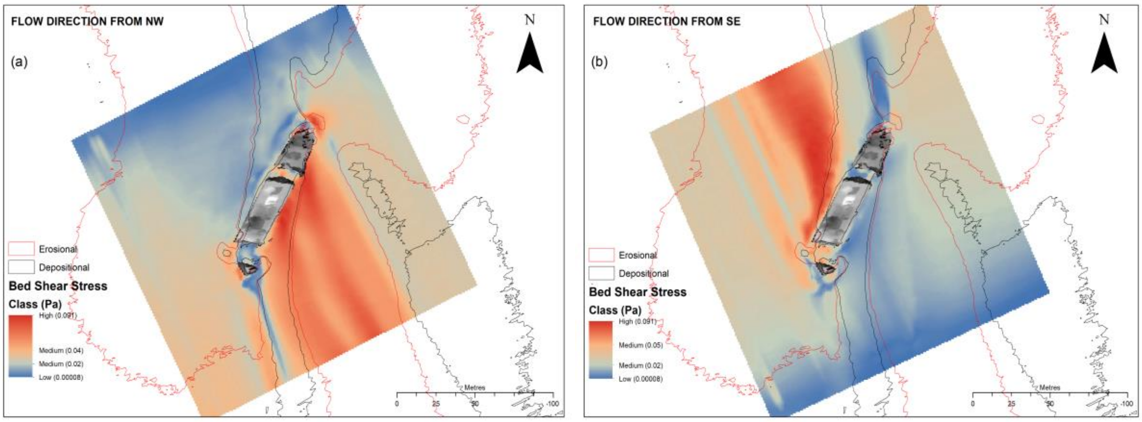

Figure 4. *Maps representing bed shear stress with flow from the NW (a) and flow from the SE (b). Red and black lines represent areas of erosion and deposition*

CFD Model Simulations and Validity: progress beyond the state of the art

The results from this study suggest that, despite a complex interaction of hydrodynamics with a seabed obstacle (i.e. a shipwreck), CFD modelling is capable of producing outputs that can be validated using real-world survey data to explain seabed sediment dynamics. Previous studies have sought to understand seabed hydrodynamics and scour through the sole use of repeat surveys or *in-situ* monitoring devices, or a combination of both (Bauri and Sarkar 2016; Majcher et al., 2020). By examining a summation of survey data, velocity values, shear stress, and flow regimes we have created a multidimensional, multipurpose model. Examination of the current velocity shows a typical flow pattern in the wreck's wake where pressure gradients created by flow around and over the wreck result in increased velocity in the centre of the wake, with less energetic flows on either side. (Quinn and Smyth, 2018). The median values of 0.1305m/s for the NW flow, and 0.1253m/s for the SE flow, reflect the slightly higher current velocities from the NW. Velocity values in the immediate vicinity of the wreck, excluding the wake areas, show an amplification of velocity when compared to the mean depth averaged velocity of 0.147m/s. Flow from the NW to SE shows an amplification factor of 2, as does flow from the SE to NW. This broadly agrees with findings from Smyth and Quinn (2014) and Whitehouse (1998), where they highlight that flow is amplified by the presence of a wreck or obstacle, including the immediate wake, by a factor of 3 to 4: an order higher than those presented here. The patterns of velocity correspond well to the patterns of shear stress, creating near mirror images. The patterns of shear stress suggest an area of erosion in the centre of the wreck's wake, with deposition on either side and where the approach flow contacts the wreck itself. This is supported by the previous survey data overlaid, showing areas of erosion and deposition by examining changes in depth. These patterns of velocity and shear stress correlate well with the overlaid survey data in that where high shear stress occurs erosion takes place, and where low shear stress occurs, deposition takes place. This serves to provide effective validation of the model. It is known however from temporal comparison of repeat survey data that the *SS Polwell* and the area adjacent do not show any signs of significant scour, typically -0.02 to -0.04 m on an interannual basis, instead suggesting a slight tendency towards deposition (Majcher et al., 2020). This is probably due to a combination of factors. Current speed in the area is considered to be relatively low in the area when compared to other shipwreck sites examined by Majcher et al. (2021) (e.g. *SS Hare*, *SS Tiberia*). With less energetic currents in the area on average throughout the year, combined with too great a depth for the wave base to interact with the seabed, the mobilisation of sediment is less likely to occur. Additionally, the presence of diurnal tides of equal magnitude would work to, at least partially, negate the mass transport of sediment outside the immediate area. The *SS Polwell* lies in a multimodal sediment, composed of gravelly muddy sand, with muddy sand further out (Figure. 1). This could have contributed to the lack of scour in that the finer mud has already been transported, or winnowed, from the area, leaving the coarser grains behind as a lag. This gravelly, muddy sand would require a higher threshold of mobilisation when compared to finer mud or sand. When examined closely, the flow patterns of the streamline models produced in OpenFOAM show that the vortices produced in the high areas of shear stress in the wreck's wake, are actually lower in velocity than the current close to the seabed. This suggests that rather than working to transport suspended sediment out of the system, the vortices enable suspension of the sediment in place. The higher velocities may exceed the mobilisation threshold, lifting the sediment into the vortex where the lower velocity cause it to dip back below the threshold, effectively resettling sediment back into to the seabed where it is lifted from again, creating a cycle until slack water signals reversal of the flow and temporarily interrupts the cycle.

Conclusions

Our study takes a novel approach, creating high-resolution models from bathymetric survey data to use as inputs in CFD simulations in OpenFOAM software. In turn, these simulations can be used to study the complex interaction between seafloor hydrodynamics and seabed objects. Modelled outputs for current flow and stress patterns correspond well with known seabed signatures for sediment erosion and deposition from survey data. The outputs from this approach can also be used in conjunction with repeat and physical (i.e. grab sample) survey data in order to understand temporal sediment dynamics and morphological change at a localised level. Ultimately this approach can be adapted and applied to other man-made structures (such as offshore wind turbine foundation structures) on the seabed as part of engineering design studies to mitigate against the risk of scour causing instability.

(ii) Implementation (milestones, deliverables, project management)

Milestones

M1: Project background review and set up complete: a thorough review of the literature was undertaken to crystalise how the objectives move beyond the state of the art. The use of CFD modelling is increasingly being used to better understand the hydrodynamic processes driving sediment transport and scour (Ahmed et al. 2015, Li et al. 2020). While many authors have used CFD modelling to analyse aspects of scour (Liu et al., 2017; Tran et al., 2015), to date there is a clear gap in the literature in the application of sediment transport models in the CFD modelling of seabed infrastructure for scour. CFD offers an innovative means to study this behaviour and predict where scour issues might occur in the future.

M2: Initial CFD modelling: a detailed modelling plan was devised to encompass an initial modelling phase, and an advanced modelling phase. To help guide this plan and ensure it's implementation, there is a weekly meeting call between myself as project supervisor, Gary as project researcher and Mark as project advisor. In this meeting progress is discussed. Issues resolved and weekly objectives set. The initial modelling plan consisted of RANS simulations based on ideas in Quinn and Smyth (2017) where the seabed is idealised as a surface with a roughness applied to it. This is a simplified approach where we would look for areas of high shear stress in our results and correlate that with areas of increased risk of scour. The plan involved creating the model in OpenFOAM software, using BlockMesh to create initial mesh and domain size. SnappyHexMesh then used to refine the mesh. Import a .stl file or .obj file that represents the geometry of the ship and the seabed terrain (this will likely be data from say 2019 that includes a scour hole). Next, apply boundary conditions to the model. For the inlet boundary condition, determine velocity profile based on data on flow/current conditions. Define the outlet as 'outlet'. Apply 'wall' boundary condition to represent the seabed. Apply a roughness coefficient to the seabed (see example from Quinn and Smyth 2017). Use 'symmetry' boundary conditions for the sides of the domain. For the top of the domain either 'slip-condition' or prescribed velocity profile (that would match the velocity at that height from inlet condition). To represent water at 10°C, assign the fluid a kinematic viscosity of 1.307m2/s. Use the solver 'SIMPLE' which is the large time-step transient solver for incompressible flow. Use the k-epsilon turbulence closer model.

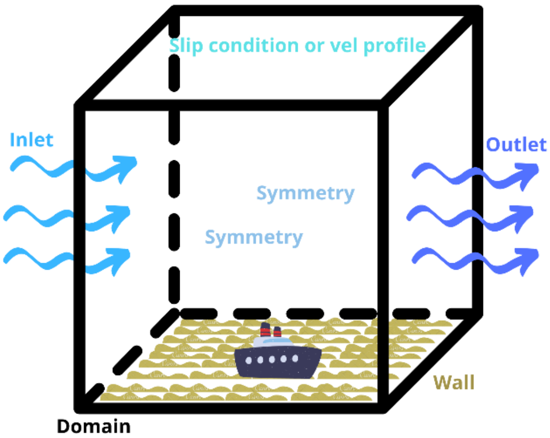

Figure 4. *Diagram representing modelling plan*

We considered how long models should run for. For example, it can take 1hr of real time to model 10 seconds of simulation. We have availed of two options for running our simulations – the UCD Sonic HPC Cluster and ICHEC. Results have been extracted from OpenFOAM and visualised using ParaView. Figure 5 below illustrations some images of the CFD model.

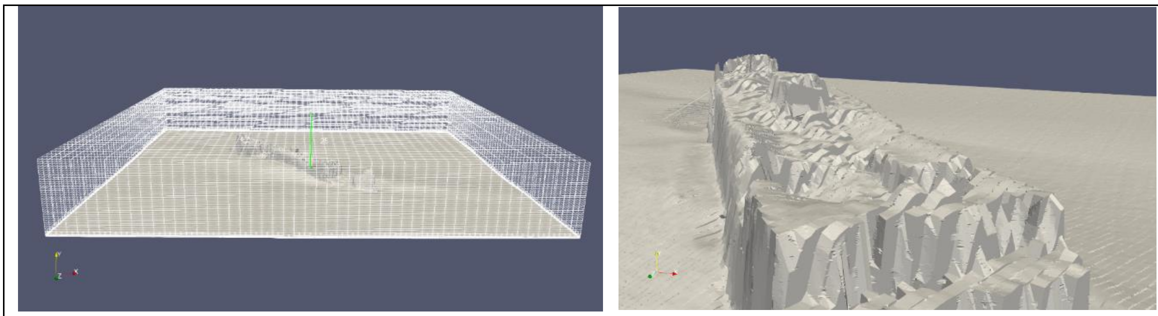

Figure 5. *Image of the CFD model*

<u>M3: CFD model results compared with repeat survey results</u>: the results have been presented earlier, and shown in Figure 3.

<u>M4: CFD model results compared with tank testing results</u>: It was not possible to complete this milestone for a number of reasons:

1. Covid restrictions made it very difficult to facilitate lab access;
2. The flume has been undergoing an upgrade and wasn't fit for purpose duing the timeframe of this project – this was supported by funding awarded to Dr Jennifer Keenahan by the UCD EQUIP call in spring 2021;

Instead of tank testing we decided it would be a more prudent use of time to model a second wreck site, which was an additional work item not planned in the original project scope. The results we achieved looking at 2 sites were significant and tank testing is definitely an area of future work we are looking to explore. To support this, Dr Jennifer Keenahan has submited a funding application to SFI to build on this work.

<u>M5: CFD model update based on field studies comparison</u>: based on the comparsion of results with repeat survey data from Milestone 3, the CFD model was improved and updated in terms of the mesh refinement and boundary conditions.

M6: CFD model results animated for outreach and dissemination: preliminary work has been completed on animating results for outreach and disseminatin. Having received reviewer comments on the journal paper submitted to the OpenFoam journal, and responded to these comments, we are awaiting the final outcome of this process. On the assumption that our paper will be publised, we will then update the animation of results and comile them into a 3min video abstract of the paper, which will be widely shared.

<u>M7: Project Workshop</u>: a workshop was planned for the 18th November which had to be postponed until the 31st March due to COVID. This will happen in the National Maritime Museum of Ireland and is in collaboration with iCRAG.

Deliverables

D1: Data Collation and Assessment: Initially, a review of existing data was performed to help inform the best choice of shipwreck for CFD modelling. It was determined that CFD models would need information on water depth, geometry of the shipwreck, geometry of the scour hole, current conditions, and seabed conditions as input parameters. In the case of the water depth, geometry of the shipwreck and geometry of the scour hole, it was determined that data in the form of a .stl file or .obj file would be best, and that this was achievable through accessing multibeam echosounder bathymetry data from INFOMAR and iCRAG. In the case of the current conditions, this data was sought in a time-series format from the Marine Institute ROMS model. For the seabed conditions (roughness values), data would be ascertained by processed grab samples from iCRAG and GSI, backscatter data through IMFOMAR and sediment classification layers through IMFOMAR. Once the above was determined as the necessary data for the project, this was cross-referenced with data available for the primary shipwreck sites in the Irish Sea (namely: SS Hare, SS WM Barkley, SS Polwell, St Michan, RMS Leinster and the HMS Vanguard). In making a decision on which site to pursue for CFD modelling, particular attention was given to whether there was repeat survey data available for sites. Based on all of the above analysis, it was decided to conduct CFD modelling for the Polwell site.

D2: Interim Report CFD Methodology and Results (Peer-review Paper 1): an initial presentation of results was made at the OpenFOAM workshop 16 conference in June 2021.

D3: Interim Report on comparison of CFD model results with field studies (Peer-review Paper 2): A full journal paper was submitted to the OpenFOAM Journal in Sept 2021. Reviews were received in Jan 2022 and revisions were re-submiteed to the journal in Feb 2022. We await the outcome of the review process.

D4: Project Workshop: a workshop was planned for the 18th November which had to be postponed until the 31st March due to COVID. This will happen in the National Maritime Museum of Ireland and is in collaboration with iCRAG.

D5: Final Report + Publication(s) prepared for peer-review submission: Gary has submitted his Thesis to UCD for examination of his Research Masters. The viva is due to take place in March 2022.

(iii) Outputs to date

(iv) Gary has presented his research work to date to his peers in the School of Civil Engineering at their regular weekly postgrad presentations.

(v) Gary has presented his work at the 16th International OpenFOAM Workshop Conference. Recording of presentation available here: https://www.youtube.com/watch?v=f7V05EqOsx8&t=10s&ab_channel=JenniferKeenahan

- Gary submitted a journal paper to the OpenFoam Journal entitled "Understanding Sediment Dynamics at a Shipwreck Site Using CFD Modelling". Reviewer comments were received and responded to. We are awaiting the final outcome of the peer review process.
- Gary has submitted an abstract to the Civil Engineering Research in Ireland Conference 2022.
- Datasets containing CFD models of the two shipwreck sites in the Irish Sea, with associated information on current velocity, flow pattern and calculated bedstress values are being prepared and will be freely available. A Data Manager will be in position in iCRAG shortly and we will liaise with them to accommodate storage of these datasets.

(iv) Impact

The primary impact of the DeMo Project has been in the areas of scientific development, training and capacity building. The project successfully built upon a number of nationally funded research initiatives including the Scour Potential Evaluation of the Western Irish Sea Mud Belt (SCOPE) project, the GIST survey, and the Geohazards and Geotechnical Engineering Spoke at iCRAG. By bringing together marine geoscientists, CFD specialists and geotechnical engineers, it allowed of the development of a novel toolkit and methodology for the characterisation of offshore sites in the context of renewable energy development and risk mitigation. It developed these approaches by using data which is freely available through the INFOMAR programme, and so demonstrated the added-value of this dataset in different engineering and environmental applications. Furthermore, the project has allowed for significant expertise development at UCD with the training of a Masters Student (Gary Littler) who is now proficient in the use of CFD modelling software, which can be applied to a number of tasks allowing him to be a creative, flexible and innovative researcher. It has also strengthened collaborative ties between researchers in engineering and applied geoscience at UCD with marine scientists and hydrographers at Ulster University, allowing for direct knowledge transfer between the various disciples and institutions. As a pilot study, the DeMo Project has been very successful in the building of capacity at UCD and facilitating growth into new research areas for iCRAG and its partners, allowing them to be competitive for further funding programmes. The project partners, in particular Project Lead Dr. Keenahan, have developed a number of funding applications based on the expertise and experience built in the DeMo project to such high-profile programmes including the IRC Government of Ireland Postgraduate Scholarship Scheme 2022 and the SFI Frontiers for the Future Programme.

<u>Publications:</u>

- Gary has presented his research work to date to his peers in the School of Civil Engineering at their regular weekly postgrad presentations.
- Gary has presented his work at the 16th International OpenFOAM Workshop Conference. Recording of presentation available here: https://www.youtube.com/watch?v=f7V05EqOsx8&t=10s&ab_channel=JenniferKeenahan
- Gary submitted a journal paper to the OpenFoam Journal entitled “Understanding Sediment Dynamics at a Shipwreck Site Using CFD Modelling”. Reviewer comments were received and responded to. We are awaiting the final outcome of the peer review process.
- Gary has submitted an abstract to the Civil Engineering Research in Ireland Conference 2022.

USING COMPUTATIONAL FLUID DYNAMICS TO MODEL AND PREDICT SEDIMENT DYNAMICS AND SCOUR IN THE IRISH SEA

SCHOOL OF CIVIL ENGINEERING
UNIVERSITY COLLEGE DUBLIN

Gary Littler 20209840

A project submitted

to University College Dublin

for the degree of

MEngSc in Civil Engineering
The School of Civil Engineering
Dr. Amanda Gibney Head of School

Supervisor: Dr. Jennifer Keenahan
Co-supervisor: Dr. Mark Coughlan

Chair/Internal Examiner: Dr. Md Salauddin
External Examiner: Dr. Thomas A.G. Smyth

7th January 2022

CONTENTS

LIST OF TABLES

LIST OF FIGURES

GLOSSARY OF SYMBOLS

β = Bed roughness coefficient
τ = Dimensional shear stress (Pa)
$\boldsymbol{\nu_{eff}}$ = effective kinematic viscosity (m^2/s)
p = Fluid density (kg/m^3)
g = Gravitational acceleration (m/s)
Z = Height (m)
U*z* = Height above seabed (m)
p = Kinematic pressure (m^2/s^2)
υ = Kinematic viscosity (m^2/s)
ω = Omega (s^{-1})
D = Particle diameter of sediment (mm)
α = Power Law
***p*s** = Sediment density (kg/m^3)
K (ν_t) = Turbulent kinetic energy (m^2/s^2)
NUT = Turbulent kinematic viscosity (m^2/s^{-1})
Ū = Velocity (m/s)
h = Water depth (m)

Acknowledgments

This project is funded by the Geological Survey of Ireland (GSI) Geoscience Research Programme under their 2020 Short Calls. Acquisition of bathymetry data was supported by the Marine Institute of Ireland's ship-time programme's APP-CV15021, CV16031: World War I shipwrecks in the Irish Sea: commemoration, visualization and heritage management and APP-CV19027: Geohazard investigation in the Irish Sea using seismic and seabed mapping techniques (GIST). The author thanks the crew of the RV Celtic Voyager on these surveys for their skill and dedication, as well as Rory Quinn, Ruth Plets, Chris McGonigle, Kieran Westley and Fabio Sacchetti for provision of data and support. The authors also express their gratitude to the MI Oceanographic Services Team for their support with ocean current data requests. Jan Majcher is supported by an Ulster University Vice-Chancellor's Research Studentship. MC is funded under an Irish Research Council Enterprise Partnership Scheme Postdoctoral Fellowship (EPSPD/2020/109) and in part by a research grant from Science Foundation Ireland (SFI) under Grant Number 13/RC/2092, with support from Gavin and Doherty Geosolutions Ltd and the Geological Survey of Ireland (GSI).

Abstract

Ireland's expansive marine resources have the potential to provide significant economic growth through the development of critical infrastructure such as offshore renewable energy installations. However, seabed hydrodynamics, morphodynamics, sediment mobility and, in particular, scour (the process of seabed erosion due to shear stresses generated by currents/waves) represent significant geological risks to the stability of such infrastructure from an environmental and engineering perspective. Such infrastructure can introduce seafloor obstacles that perturb the local environment inducing scour that can cause structural instability, or deposition resulting in the burying of structures. Understanding the processes that drive these complex patterns of sediment erosion and deposition over varying timescales is critical to the sustainable development of critical offshore infrastructure. Traditionally, assessments for such issues have utilised time-lapse bathymetric surveys and scaled physical testing. The former fails to capture the nuance of these processes between data collection surveys and cannot predict how the seabed will react to an obstacle, whilst the latter is costly and limited in recreating the marine environment. Predicting scour can be difficult due to vagaries about hydrodynamic conditions. Computational Fluid Dynamics (CFD) is an advanced modelling technique that solves problems of fluid flow and offers an effective means of investigating the complex interaction between hydrodynamics and manmade objects on the seafloor. Similarly, shipwrecks offer natural laboratories with which to validate models using CFD approaches. In this thesis, CFD simulations are generated for a high-resolution bathymetric survey dataset of two shipwreck sites and assessed for application in future scour prediction studies. Shipwrecks offer novel *in-situ* features with which to test theories of hydrodynamics and sediment transport around seabed objects, with CFD modelling offering a robust tool to do so. The aim of this thesis is to develop a CFD model at a shipwreck site in order to simulate current flow patterns and magnitudes with which to better understand seabed morphological patterns of sediment erosion and deposition caused by the wreck's obstruction. When combined with other high-resolution seabed survey data, these outputs and understandings could potentially be applied to other critical offshore engineering as part of a robust methodology to assess the impacts of sediment dynamics and prevent scour and other adverse impacts. Modelled outputs for current flow and stress patterns correspond well with known seabed signatures for sediment erosion and deposition from survey data. The outputs from this approach can also be used

in conjunction with repeat and physical (i.e. grab sample) survey data in order to understand temporal sediment dynamics and morphological change at a localised level. Ultimately, this approach can be adapted and applied to other man-made structures (such as offshore wind turbine foundation structures) on the seabed as part of engineering design studies to mitigate against the risk of scour causing instability.

I hereby certify that the submitted work is my own work, was completed while registered as a candidate for the degree stated on the Title Page, and I have not obtained a degree elsewhere on the basis of the research presented in this submitted work

1 Introduction

Globally, investment in 'green' energy sources is rising rapidly, with a view to move away from traditional energy sources such as fossil fuels. Action to reduce carbon emissions globally through international meetings such as COP26 shows a desire at an international level to move towards carbon neutrality. This is being put into action on a national scale by legislation such as Ireland's Climate Action and Low Carbon Development Bill, designed to decarbonise Ireland's energy production, and recognising offshore wind power as a vital area of investment. In moving towards carbon neutral energy sources, offshore technologies such as wind farms (Figure 1) are seen as a critical area of investment.

Figure 1. ***Rampion Offshore Wind Farm***

When siting individual offshore wind turbines, seabed sediment mobility and the potential for scour development is a significant geohazard and environmental constraint associated with the development of this sector, in addition to other engineering infrastructure such as cables and pipelines (Mellet et al., 2015). Scour is the process in which sediment is eroded and transported due to an imposed shear stress generated by seabed current and/or waves. Its effects have been widely reported, documented, and examined (Quinn, Bull and Dix, 1997; Bauri and Sarkar 2016; Schendel et al., 2018). The rate of sediment erosion is largely dependent on the energy generated by local flow regimes and the properties of the sediment on the seabed.

Whilst scour is a naturally occurring phenomenon, the introduction of man-made obstacles onto the seabed can magnify the effects due to an increase in bed shear stress. This is caused by pressure differences created by fluid flow being redirected over and around the obstacle, increasing flow velocity and turbulence. Over time this can lead to the formation of scour holes around the obstacle where shear stress is highest. As the energy and turbidity of the flow decreases it loses its ability to transport suspended sediment in the water column, leading to deposition. These scour holes can lead to damage and destabilisation of structures such as turbine foundations and "free-spanning" of cables, requiring concerted efforts to remediate existing damage and prevent further scour from occurring. To mitigate the effects of scour, seabed defences such as rock armour can be utilised after initial installation, and have been extensively examined (Vos et al., 2011, 2012; Ma and Chen, 2021). These can be technically difficult to implement however and are usually installed only after the effects of scour have been identified, leading to increased costs. Arklow Bank, Ireland's only offshore wind farm constructed to date, experienced scour issues (Figure 2) that had a significant impact on the project, resulting in the use of rock armour in an attempt to mitigate against further scour and turbine instability (Whitehouse et al., 2011). Therefore, anticipating such issues and strategically placing defences, or avoiding high shear stress areas altogether, can increase the viability and longevity of installations. Based on experiences across Europe, there is a significant amount of focus on geotechnical assessments for scour and related processes in relation to offshore engineering and mitigation (Matutano et al., 2013). Efforts to understand sediment dynamics and scour evolution using repeat survey techniques alone can be challenging, as observations often require visual interpretation of the seabed features and their effect on the flow regime (Quinn, Bull and Dix, 1997), without detailed examination of the current flow dynamics. This can lead to an element of subjectivity. These methods can be costly, time-consuming, and provide an incomplete understanding of the factors at work due to the large scale of the task. Other methods include small laboratory-based modelling (Schendel et al., 2018), larger models contained in specialised facilities (Welzel et al., 2019), or specialized full-scale experiments such as that performed by Ma and Chen (2021) on the National Renewable Energy Laboratory (NREL) wind turbine in the United States. There are, however, significant limitations imposed on these methods. Scaling down models introduces unavoidable errors due to the loss of real-world variables. Full scale test models still suffer from difficulty recording measurements, although to a lesser extent than their real-world counterparts, and conditions such as the weather can hinder prospective studies. Devices to monitor conditions *in-situ* must be subjected to varying conditions and are at risk of failure, leading to data gaps and increased costs to repair them. In general, there is a clear need for a better understanding of localised seabed dynamics and subsequent impacts on morphodynamics and scour development. However, there is a paucity of direct observations and data on scour development processes.

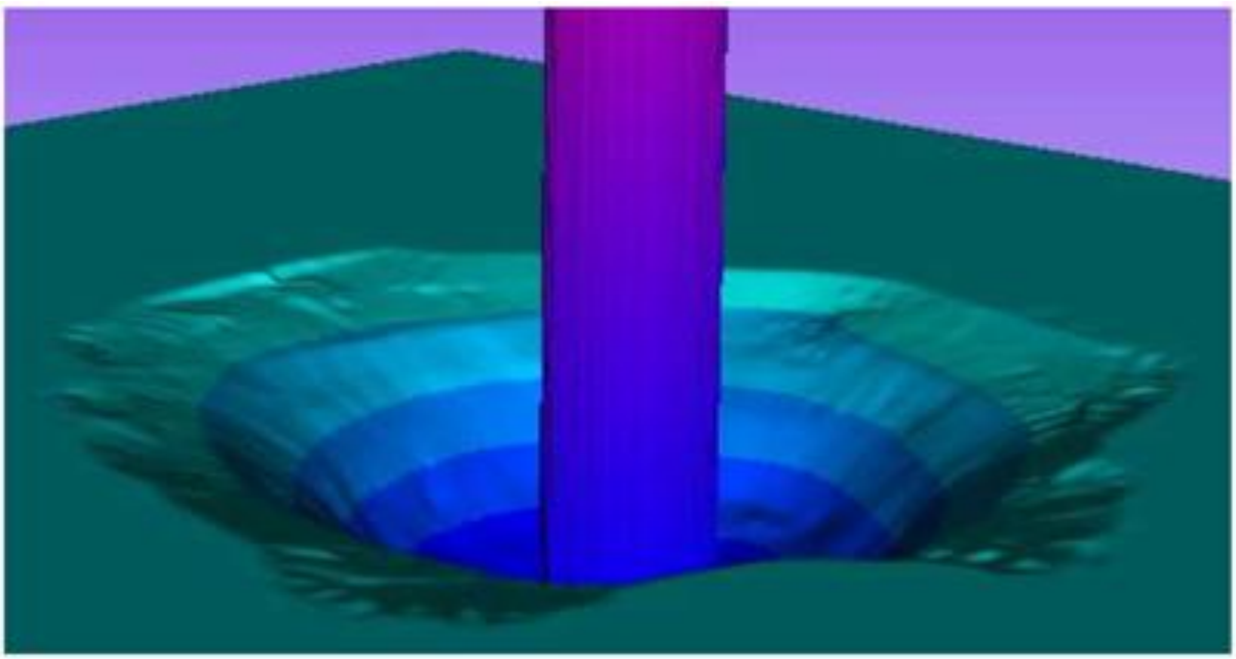

Figure 2. ***Scour hole measured at Arklow Bank shortly after installation (from Whitehouse et al., 2011)***

Computational Fluid Dynamics (CFD) is a tool used to model fluid flow in specific situations and can be used to model a section of the seabed, along with any obstacles within with respect to current flow dynamics. The application of CFD modelling can further enhance the understanding of hydrodynamic processes driving sediment transport and scour (Li, Ong and Fuhrman, 2020). Using a solver based on Navier-Stokes equations, fluid flow can be simulated and its interaction with obstacles analysed. Smyth and Quinn (2014), Quinn and Smyth (2017), and Fernández-Montblanc et al., (2018) demonstrated how CFD modelling applied over a shipwreck site could garner significant insight into the hydrodynamic regime, including interaction with seafloor sediments, providing an understanding of scour signature formation processes. Typically, the siting of offshore renewable energy infrastructure, such as wind turbines, deliberately avoids shipwrecks on the seabed, as they are protected and highly significant archaeological locations. However, they are being studied as natural seabed laboratories to examine the complex interaction of man-made objects, seafloor sediment transport and hydrodynamic processes (Majcher et al., 2021). These man-made obstructions provide a temporal representation of an obstacle on the seabed, capable of disrupting the otherwise natural flow regimes present on a local scale. Modern remote sensing techniques can provide extremely high-resolution imaging, in tens of cm, enabling highly detailed studies to be performed using shipwrecks as a proxy for other artificial and natural obstructions.

When combined with these repeat hydrographic surveys that provide high-resolution bathymetric data detailing seabed geomorphic change, CFD is a powerful tool to elucidate patterns of turbulent flow and enhanced currents around seabed obstructions at a localised scale. Turbulence models can also be utilised to increase the accuracy of the model in complex systems, allowing for more detailed analyses of the flow. By using an approach based on CFD it is possible to produce an accurate prediction model for scour on a large spatial scale without the complexities of *in-situ* modelling. For example, Yang et al., (2021) utilised the commercial CFD software ANSYS Fluent in order to determine the effectiveness of a submerged tidal current turbine (TCT) for scour mitigation and extra green energy production. CFD enabled the identification of a need for the correct positioning of the TCT at the base of the monopile for optimum performance. When used in conjunction with real-world measurements, its effectiveness can be increased even further through verification and validation. CFD also represents a lower cost solution compared with conventional survey and experimental methods (Tolias et al., 2019), being desk-based and able to run on open-source software.

The ability to accurately predict and quantify areas of high shear stress potentially occurring around structures using real-world conditions such as flow velocity, turbulence, and sediment type, can help inform the planning of installations regarding location, engineering, and design. De-risking potential sites is of vital importance for the renewable energy sector, in terms of both running costs and insurance. Gatzert and Kosub (2016) classify several risk factors involved in renewable energy project planning, from strategic/business risks such as financing risks and insufficient public acceptance to liability/legal risks. Scour falls under operation/maintenance risks, spanning general operation and maintenance, damage due to natural hazards, and revenue loss due to business interruption. In short, higher risk factors in renewable energy projects can lead to increased running costs, hindering the progress of such projects or rendering them unfeasible to investors. In terms of physical hazards, mitigation methods could be better adapted to suit the specific area for siting offshore renewable technology at an early stage in the development process. CFD modelling provides an effective tool for analysing and de-risking projects early in the planning phase, by providing a foresight into the conditions affecting renewable energy infrastructure sites.

Shipwrecks offer novel *in-situ* features with which to test theories of hydrodynamics and sediment transport around seabed objects when analysed using CFD. Smyth and Quinn (2014) provided the basis for CFD modelling of shipwrecks' flow behaviour and further developed their approach to model flow development, erosion, and deposition using a generic 3-D wreck model and idealised seabed surface. The aim of this thesis is to further develop this technique by creating a CFD model using representations of real-world shipwreck sites and conditions, in order to simulate current flow patterns and magnitudes. This can further our understanding of seabed morphological patterns of sediment erosion and deposition caused by the wreck's obstruction by examining multiple factors, where previous methods focused on one at a time. When combined and compared with other high-resolution seabed survey data, these outputs and understandings could potentially be applied to other critical offshore engineering as part of a robust methodology to assess the impacts of sediment dynamics and prevent scour and other adverse impacts. Two shipwreck sites will be modelled and assessed, in order to provide a comparison of contrasting conditions. These sites were chosen from the many available off the coast of Ireland based upon certain 'suitability factors' that made them suitable as proxies for modelling. Both wrecks will be presented as case studies and modelled within OpenFOAM-v2012, with individual flow patterns and bed shear stress quantified and compared with each other and against repeat survey data. Patterns of erosion/deposition will be examined and discussed. Finally, a fully replicable, validated CFD model of seabed flow and bed shear stress around an object will be established.

In chapter one the topic of scour and its relevance to renewable energy projects and their importance is presented. The use of shipwrecks as a proxy for seabed infrastructure and the application of CFD using these wrecks is outlined. In chapter two the chosen shipwreck sites will be presented. The data sources and acquisition techniques will be outlined. The two case studies (shipwrecks) will be presented in detail with their seabed characteristics and dominant current flow. In chapter three the methodological framework will be outlined. Conditions of the model, the numerical modelling techniques, and solver used will be explained. The individual model conditions will be outlined for the two case studies. In chapter four the model results will be outlined. Flow regimes will be examined for both cases as will erosional and depositional signatures for validation of the model. In chapter five the results are discussed. The two cases are compared, the model methodology is explained, and its limitations and possible future methods are considered. In chapter six conclusions are presented, achievements are considered.

2 Shipwreck Sites

To best represent the effect of an obstruction such as a monopile wind turbine foundation on seabed flow dynamics and potential scour development, shipwreck sites in the Irish Sea were identified as ideal natural laboratories. Using repeat survey data, a long-term record of seabed morphodynamic development in the area local to the wreck can be used as a validation tool for developed CFD models.

2.1 Description of the Sites

Two sites were chosen as part of this study based on three main factors:

1. Location, i.e. in the Irish Sea;
2. Composition of seabed sediment at the wreck and surrounding area. The wreck must be located in sediment with potential for mobilisation such as sand or mud;
3. Data availability:
    a. Data must be available for bathymetry, ground truthing (grab samples), current magnitudes and frequency;
    b. Data for possible scour development identification must be available to compare against. Areas of historical erosion/deposition will be used as a reference for verification.

Based on the above parameters the shipwrecks *SS Polwell* and *SS Hare* were chosen (Figure 3).

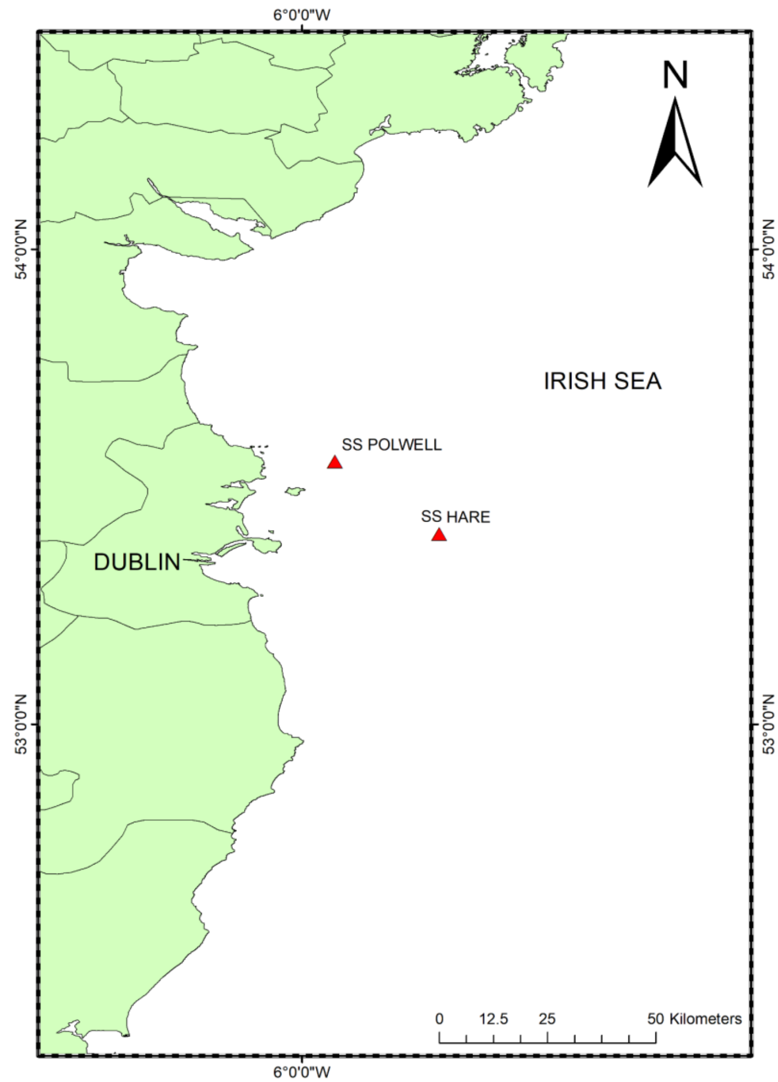

Figure 3. Location of chosen wrecks SS Polwell and SS Hare in the Irish Sea, off the coast of Dublin

Two wrecks were chosen in order to build upon techniques and methods from the first to the second, to compare and contrast the cases, and to provide validation of the model through the use of more than one case study. Seabed characteristics and current parameters for both sites were identified (Table 1). The *SS Polwell* was chosen initially as it met additional conditions required for turbine monopile installation, including a suitable depth (50 m cutoff for monopile foundations), it was not located within a Marine Protected Area (MPA), it was not within a current or planned installation, and also not located directly in a major shipping or ferry route. This was to provide an overview of the conditions associated with an ideal installation site. The

SS Hare was chosen solely based on the three factors mentioned previously, and to provide a contrast with the *SS Polwell* in terms of current speed.

Other shipwrecks were considered but eliminated as options:

- SS Chirripo, SS Tiberia, SS Lugano, SS Santa Maria - Outside the area of interest (Irish Sea);
- RMS Leinster, HMS Vanguard, FV St Michen - Insufficient or less time-lapse survey data compared with the two chosen wrecks.

Table 1. ***Table showing mean current speed and seabed characteristics for both shipwrecks based on repeat survey data and physical sediment (grab) sampling***

	SS Polwell	SS Hare
Mean Current Speed (m/s)	0.147	0.23
Water Depth Range (m) (Deepest and shallowest points on the seabed and wreck)	10 (26 - 36)	17 (49 - 66)
Sediment Type	Multimodal (muddy sand, gravelly muddy sand)	Sand
Local Bedforms	Ridges to south	Large sediment waves
Prevailing current direction	North-west to south-east	North-west to south-east

2.2 Data Acquisition

Both shipwrecks have already been investigated as part of other studies (Westley et al., 2019; Majcher et al., 2021). Repeated high-resolution bathymetric data has been collected at the *SS Polwell* and *SS Hare* sites aboard the *RV Celtic Voyager* as part of three separate surveys in 2015 (CV15021), 2016 (CV16031) and 2019 (CV19027) under the Marine Institute Ship-Time Programme, allowing for detailed and general site characterisation. In this thesis, bathymetric data collected as part of the CV19027 survey was used. The multibeam echosounder (MBES) data were acquired using a dual-head, hull-mounted Kongsberg EM2040 operating at 400 kHz, with a continuous wave pulse. An integrated GNSS/L-Band receiver CNAV 3050 provided primary position corrections, and a Seatex Seapath 330+ acted as a secondary positioning system as well as providing motion referencing and timing. Survey lines were aligned in a grid, which allowed for 110°- 120° swath coverage. Data from the 2019 survey were cleaned and processed in Caris HIPS and SIPS v. 9 using the the Combined Uncertainty and Bathymetry Estimator algorithm (CUBE; Calder & Wells, 2006), and were tidally corrected before being exported as digital elevation models (DEMs) as raster format in the UTM 30N projection. The horizontal resolution of this dataset is 0.2 m. More details on all data processing and compliance with IHO Special Order standards can be found in Majcher et al. (2020; 2021). DEM rasters were used as geometry input for CFD modeling efforts.

2.3 Case Study 1 (SS Polwell)

The *SS Polwell* is located approximately 10 km off the east coast of Ireland, north of Dublin, in the Irish Sea (Figure 4). It originally measured 86.56 x 11.6 x 5.53 metres and operated as a defensively armed steam collier. It was torpedoed by a German submarine on 5th June, 1918 with no loss of life. The wreck lies in approximately 29.8 m water depth, orientated NE-SW with the bow to the NE, on seabed comprising a multimodal distribution of sediment types (Majcher et al., 2021). Ground-truthing grab samples taken from the site suggest muddy sand and slightly gravelly muddy sand. To the south of the *SS Polwell* are a several seabed ridges believed to be out-cropping bedrock or glacial till. Approximately 600 m to the north of the *SS Polwell* site a gas interconnector pipeline transverses east-west. Previous residual relief modelling highlighted extensive erosional and depositional features to the north of the site, with limited development to the south due to the presence of the seabed ridges (Majcher et al., 2020). Modelled data for seabed currents in the area suggest a dominant NW-SE direction of flow reaching a maximum of 0.4 m/s.

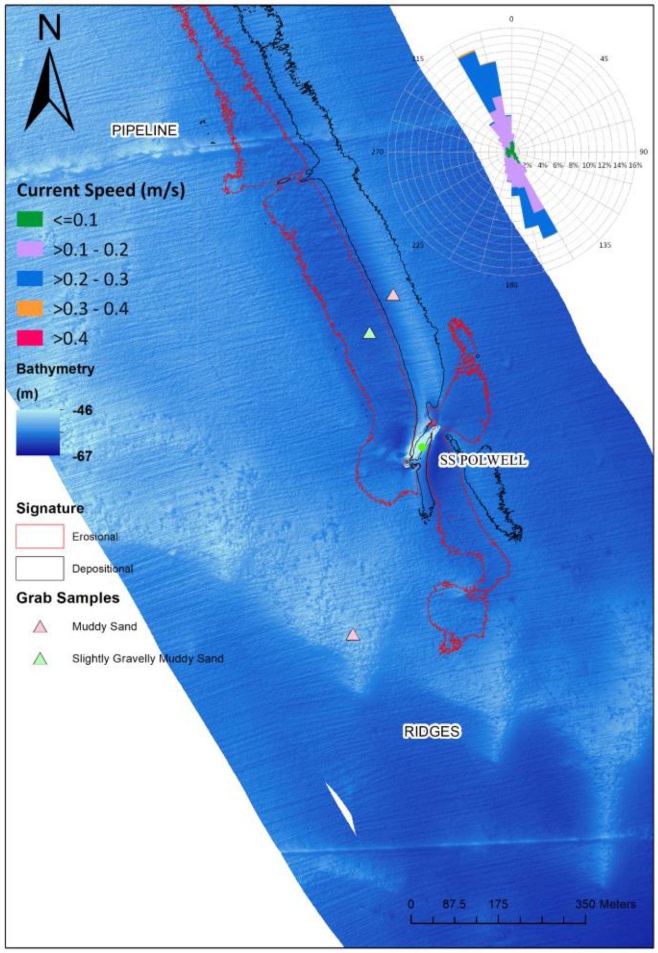

Figure 4. Location of the SS Polwell in the Irish Sea and site characterisation. Rose chart (top right) represents modelled data for near-seabed currents. Bathymetry data is presented with a hillshade effect (azimuth 315°, elevation 45°). Seabed signatures are delineated according to the approach of Majcher et al. (2020). Grab sample locations are represented by coloured triangles

2.4 Case Study 2 (SS Hare)

The *SS Hare* is located around 22 km off Howth Head Peak, North of Dublin in the Irish Sea (Figure 5). It originally measured 65.8 x 9 x 4 metres and operated as a merchant steamship. It was torpedoed by a German submarine on 14th December, 1917 with the loss of twelve lives. The wreck lies in approximately 60 m water depth, orientated NE-SW with the bow to the SW, on seabed comprising non-cohesive sandy sediments (Majcher et al., 2020). Grab samples taken from the site show the presence of sand and gravelly sand inside the scour pit in which the wreck lies, with previous studies finding high volumes of sediment eroded here (Majcher et al., 2021). The area surrounding the pit is populated by bifurcating sediment waves superimposed on larger sediment waves, around 7 m high. Modelled data for seabed currents in the area suggest a dominant NW_SE direction of flow reaching a maximum of 0.51 m/s.

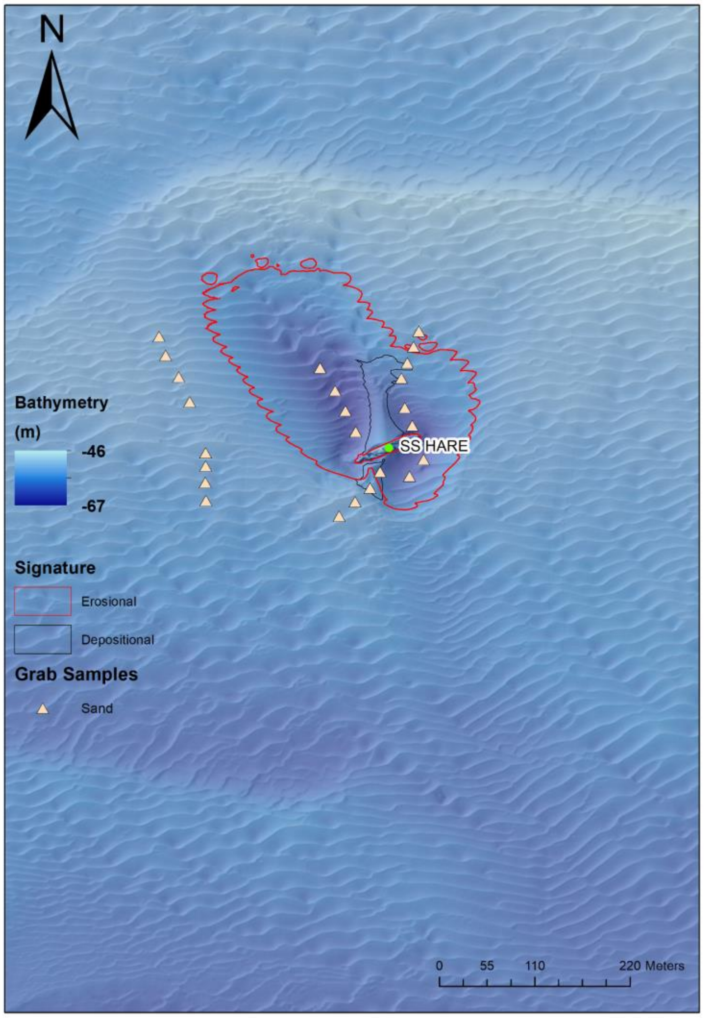

Figure 5. Location of the SS Hare in the Irish Sea and site characterisation. Rose chart (top right) represents modelled data for near-seabed currents. Bathymetry data is presented with a hillshade effect (azimuth 315°, elevation 45°). Seabed signatures are delineated according to the approach of Majcher et al. (2020). Grab sample locations are represented by coloured triangles

3 CFD Modelling Methodology

Figure 6 presents an overview of the CFD modelling methodology used in this thesis. The following sections in this chapter present the boundary conditions governing equations, solver, geometry, computational domain, and computational mesh used for both case studies.

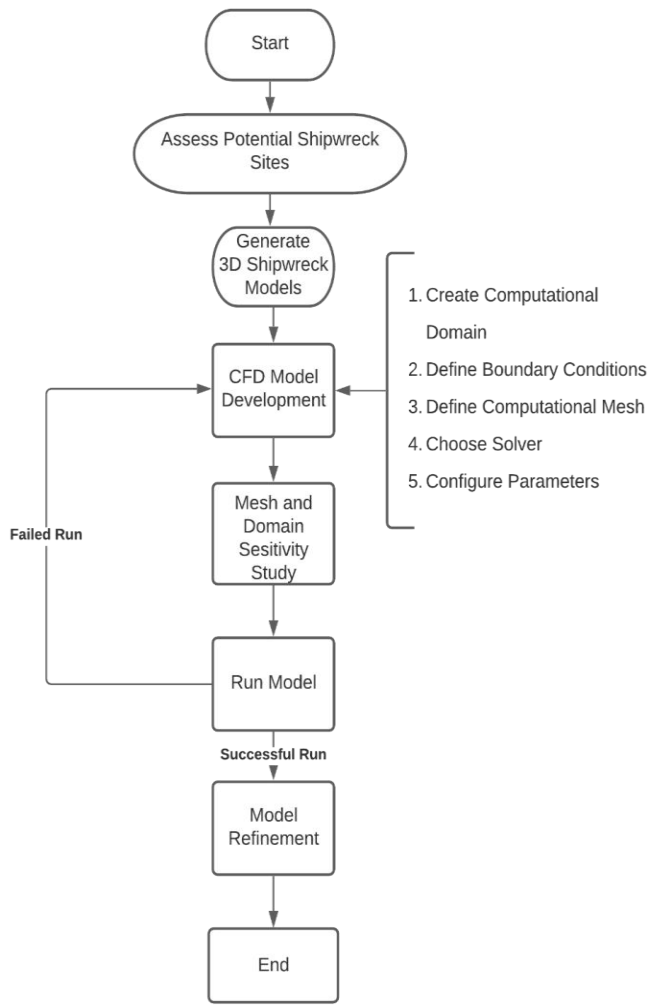

Figure 6. *Flow chart with operational order*

3.1 Boundary Conditions

The boundary domain (Figure 7) consisted of six faces, with fluid flow moving from the inlet to the outlet. Inlet and outlet boundary conditions were created at opposite sides to define a flow direction, with the geometry oriented to represent the prevailing current. The patch types assigned to each of the six faces are shown in Table 1.

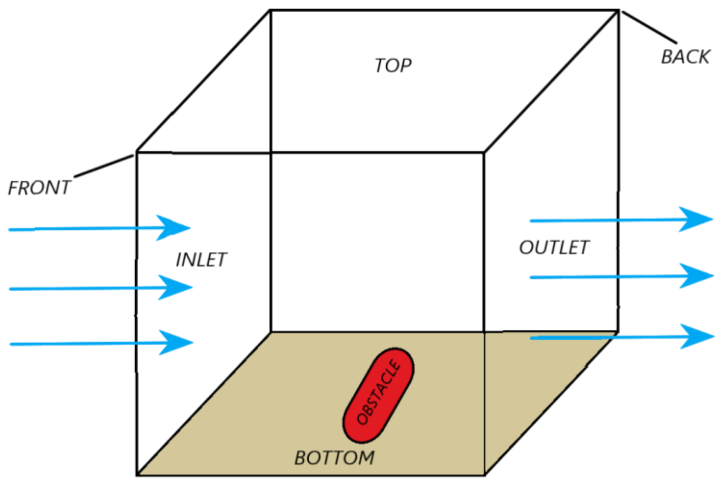

Figure 7. *CFD model setup showing boundary types. Brown represents seabed, blue arrows represent flow direction*

Table 2. *Setup of patch types for boundaries in blockmesh*

BLOCKMESH BOUNDARY FACE	***PATCH TYPE***
INLET	*PATCH*
OUTLET	*PATCH*
TOP	*SLIP*
BOTTOM	*WALL*
FRONT/BACK	*SYMMETRYPLANE*

A power-law velocity profile was generated at the inlet for U by using the equation described in Soulsby (1997) and Lewis et al. (2017):

$$Uz = \left(\frac{z}{\beta\, h}\right)^{\frac{1}{\alpha}} \bar{U} \qquad (1)$$

Where the velocity profile (the velocity at height ***Z*** above the seabed **Uz**) is described using a power law (**α**) and bed roughness coefficient (***β***), with water depth (**h**) and depth averaged velocity (**Ū**). Current data for the *SS Polwell* and *SS Hare* was obtained from the Marine Institute of Ireland using output from their operational hydrodynamic model (Nagy et al., 2020), which is run on the Regional Ocean Modeling System (ROMS: Shchepetkin and McWilliams, 2005). Data was obtained for depth-averaged current velocity and direction for a 1-year period and used in site characterisation (see current speed rose Figure 4, 5) and as inlet current speed values in CFD modelling efforts. $\bar{\mathbf{U}}$ was prescribed a value using the average for the year's recorded values, 0.147 m/s for the SS Polwell, 0.23 m/s for the *SS Hare*, at 1 m from the seabed**.** This was the most effective method for generating $\bar{\mathbf{U}}$ however, it does not account for outliers of excessively large and small values and may be skewed by them to some extent. Values were generated using the above formula and entered into a .csv file for use with the OpenFOAM *fixedProfile* boundary condition. A summary of the boundary conditions of the five primary unknowns (U, p, k and ω and nut) applied at each boundary region is shown in Table 3.

Table 3. *Boundary conditions of simulations based on the k-ω SST model*

	P	***U***	***K***	**ω**	***NUT***
DIMENSIONS	*[0 2 -2 0 0 0 0]*	*[0 1 -1 0 0 0 0]*	*[0 2 -2 0 0 0 0]*	*[0 0 -1 0 0 0 0]*	*[0 2 -1 0 0 0 0]*
UNITS	m^2/s^2	*m/s*	m^2/s^2	s^{-1}	m^2/s^{-1}
INTERNALFIELD (SS POLWELL)	*UNIFORM 0*	*UNIFORM (0 0 0)*	*UNIFORM 0.000013*	*UNIFORM 0.00206*	*UNIFORM 0*
INTERNALFIELD (SS HARE)	*UNIFORM 0*	*UNIFORM (0 0 0)*	*UNIFORM 0.00003174*	*UNIFORM 0.00123*	*UNIFORM 0*
INLET	*ZEROGRADIENT*	*FIXEDPROFILE*	*FIXEDVALUE;* *VALUE $INTERNALFIELD*	*FIXEDVALUE;* *VALUE UNIFORM 1*	*CALCULATED;* *VALUE UNIFORM 0*
OUTLET	*FIXEDVALUE;* *VALUE UNIFORM 0*	*ZEROGRADIENT*	*INLETOUTLET;* *INLETVALUE $INTERNALFIELD;* *VALUE $INTERNALFIELD*	*INLETOUTLET;* *INLETVALUE $INTERNALFIELD;* *VALUE $INTERNALFIELD*	*ZEROGRADIENT;*
TOP	*SLIP*	*SLIP*	*SLIP*	*SLIP*	*SLIP*
BOTTOM	*ZEROGRADIENT*	*ZEROGRADIENT*	*KQRWALLFUNCTION;* *VALUE $INTERNALFIELD*	*ZEROGRADIENT*	*NUTKWALLFUNCTION;* *VALUE UNIFORM 0*
FRONT/BACK	*SYMMETRY*	*SYMMETRY*	*SYMMETRY*	*SYMMETRY*	*SYMMETRY*
POLWELL/HARE *(PATCH APPLIED TO SEABED AND WRECK GEOMETRY)*	*ZEROGRADIENT*	*NOSLIP*	*KQRWALLFUNCTION;* *VALUE $INTERNALFIELD*	*OMEGAWALLFUNCTION;* *VALUE $INTERNALFIELD*	*NUTKWALLFUNCTION;* *Ks UNIFORM 0.000755;* *Cs UNIFORM 0.5;* *VALUE UNIFORM 0*

3.2 Governing Equations

In the presented CFD models, the flow within the testing domain is assumed to be incompressible, Newtonian, and statistically steady, with temperature and gravity effects neglected. The flow is governed by the Reynolds-Averaged Navier-Stokes (RANS) formulation for mass and momentum:

$$\nabla \cdot \mathbf{U} = 0$$
$$\nabla \cdot (\mathbf{UU}) = \nabla \cdot [\nu_{eff} (\nabla \mathbf{U} + (\nabla \mathbf{U})^T)] - \nabla p \quad (1)$$

Where **U** is the time-averaged velocity, p is the time-averaged kinematic pressure (pressure divided by density), ν_{eff} is the effective kinematic viscosity which is the summation of laminar kinematic viscosity (ν) and the turbulent kinematic viscosity (ν_t). The value of ν is 1.307×10^{-6} m^2/s, representing water at (10 °C). The unknown ν_t is calculated from the turbulent kinetic energy (k) and the energy dissipation frequency (ω) using the k-ω SST (shear stress transport) turbulence model due to its ability to solve, in detail, at both the boundaries and the internal field.

3.3 Solver

In this study, the RANS simulations employ the SIMPLE algorithm to perform the pressure-velocity coupling (simpleFOAM solver in OpenFOAM-v2012). It is a steady state solver for incompressive, turbulent flow. Simulations for the SS Polwell were run locally on a single machine through Windows Subsystem for Linux. Due to the file size and the computational complexity of the SS Hare's geometry and domain, simulations were performed using UCD's Sonic Cluster, a high-performance computing (HPC) cluster designed to deal with complex tasks using parallel processing over a number of nodes (multiple machines linked together).

For the *SS Polwell*, flow from the NW achieved convergence in 1164 iterations (seconds) and the SE flow converged in 773 iterations. For the SS Hare, flow from the NW did not converge automatically but was allowed to run for 50,000 iterations where convergence was recognised, as the flow no longer showed signs of evolution. The SE flow converged in 324 iterations.

3.4 Geometry

3.4.1 SS Polwell

The geometry of the seabed and wreck of the SS Polwell were contained within a point cloud .asc file, with both being part of a singular datafile, as opposed to separate samples. This data was gathered as part of the CV19027 Survey, at a resolution of 0.2 m. This file was then converted into a stereolithography (.stl) file to provide a 3-dimensional representation (Figure 8), as well as compatibility with OpenFOAM v_2012. In order to accurately represent the correct flow direction, the .stl file was processed in Blender version 2.92.0 and rotated to align with the dominant north-westerly flow. This was repeated for the south-easterly current direction to provide an accurate representation of flow in a bidirectional current system. The seabed geometry was placed at point 0 on the z axis of the domain, 10 m above the base of the mesh to avoid interference where the dips in the seabed would cross outside the computational domain. The seabed and wreck geometry were prescribed a predefined roughness length (Z_0) of 0.06 m, representing rippled sand, as used by Quinn and Smyth (2017).

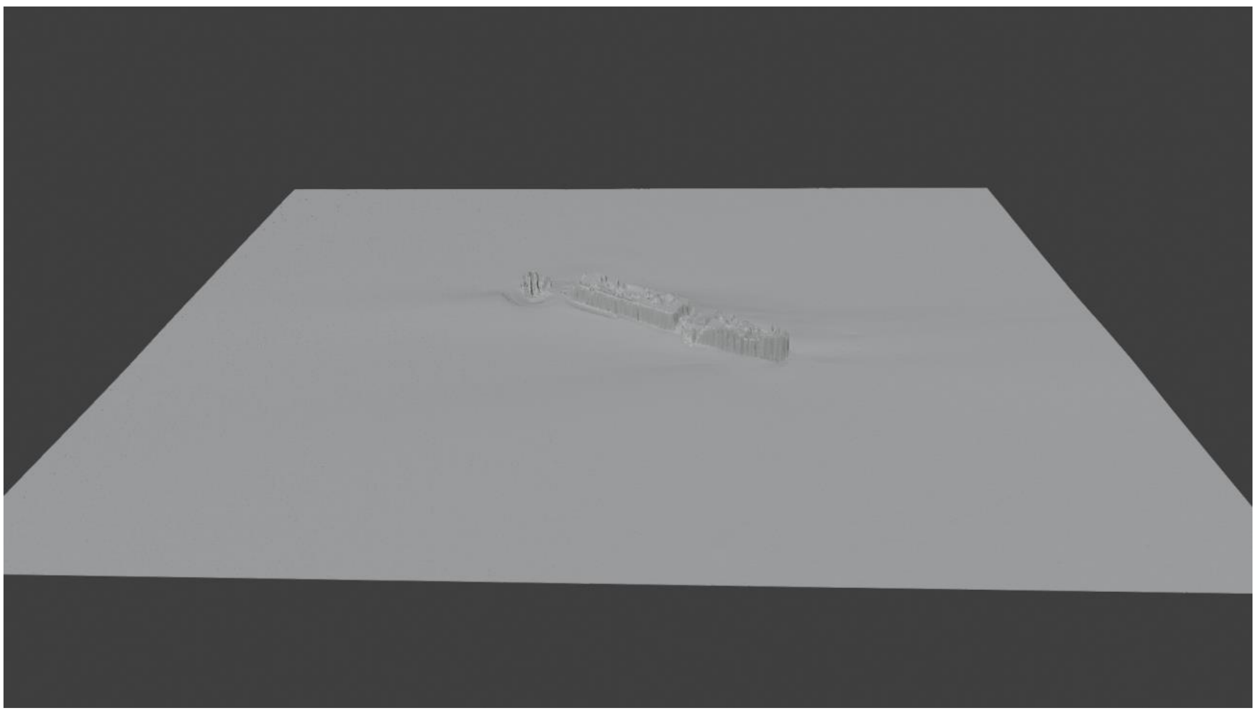

Figure 8. *3-Dimensional model of the SS Polwell and surrounding seabed, rendered in Blender v-2.92.0*

3.4.2 SS Hare

As with the *SS Polwell*, the seabed and wreck geometry for the *SS Hare* were contained within a singular point cloud .asc file. This data was gathered as part of the CV19027 survey, at a resolution of 0.2 m. The file was then converted into a .stl file (Figure 9). To represent the correct flow direction, the .stl file was processed in Blender version 2.92.0 and rotated to align with the dominant north-westerly flow. This was repeated for the south-easterly current direction to provide an accurate representation of flow in a bidirectional current system. The seabed geometry was placed at point 0 on the z axis of the domain, 10 m above the base of the mesh to avoid interference where the dips in the seabed would cross outside the computational domain. To be consistent with the *SS Polwell*, the seabed and wreck geometry were also prescribed a Z_0 value of 0.06 m for rippled sand (Quinn and Smyth, 2017).

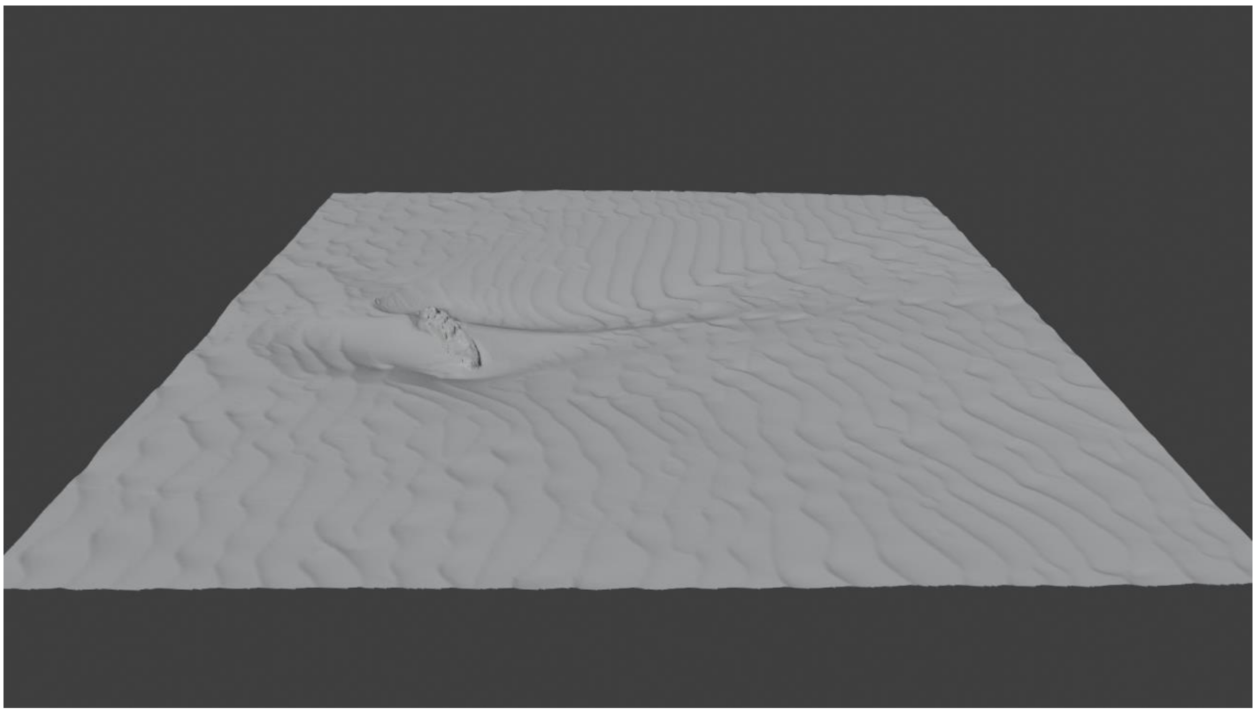

Figure 9. *3-Dimensional model of the SS Hare and surrounding seabed, rendered in Blender v-2.92.0*

3.5 Computational Domain

3.5.1 SS Polwell

The cuboidal computational domain for the *SS Polwell* represents a length of 100 m, a width of 100 m and a depth of 35 m (Figure 10). The actual domain descends a further 10 m vertically from the 3D geometry, which is situated at 0 m, giving a Y axis value of -10 m to +25 m. This was required as the natural undulations on the seabed caused it to dip below 0 m when the domain was given a Y value of 0 to +25 m., exposing the base of the mesh and introducing interference into the model. The *SS Polwell* lies at a depth of 29.8 m however, the surface of the sea is a dynamic and changing environment. The 4.8 m excluded from the natural domain provides a buffer where tidal and wave induced influences might occur.

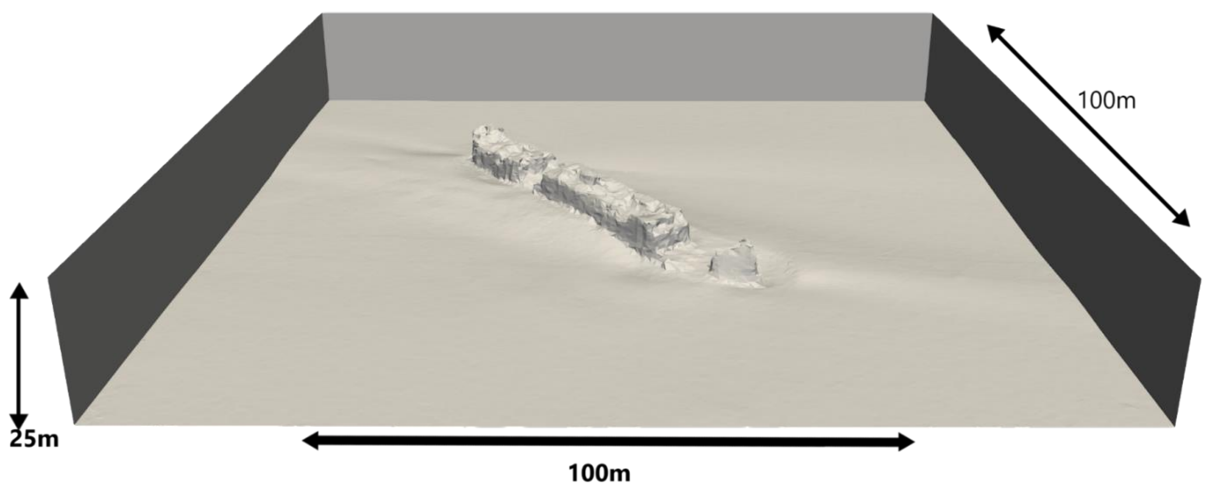

Figure 10. *Computational domain for the SS Polwell*

3.5.2 SS Hare

The cuboidal computational domain for the *SS Hare* represents a length of 290 m, a width of 270 m and a depth of 75 m (Figure 11). The actual domain descends a further 10 m vertically from the 3D geometry, which is situated at 0 m, giving a Y axis value of -10 m to +65 m, consistent with the *SS Polwell* to avoid parts of the seabed being excluded from the base of the domain. The *SS Hare* was not provided a surface buffer as it was deemed unnecessary due to the larger depth of the domain. Any surface interactions would have a negligible effect at a depth of 65 m.

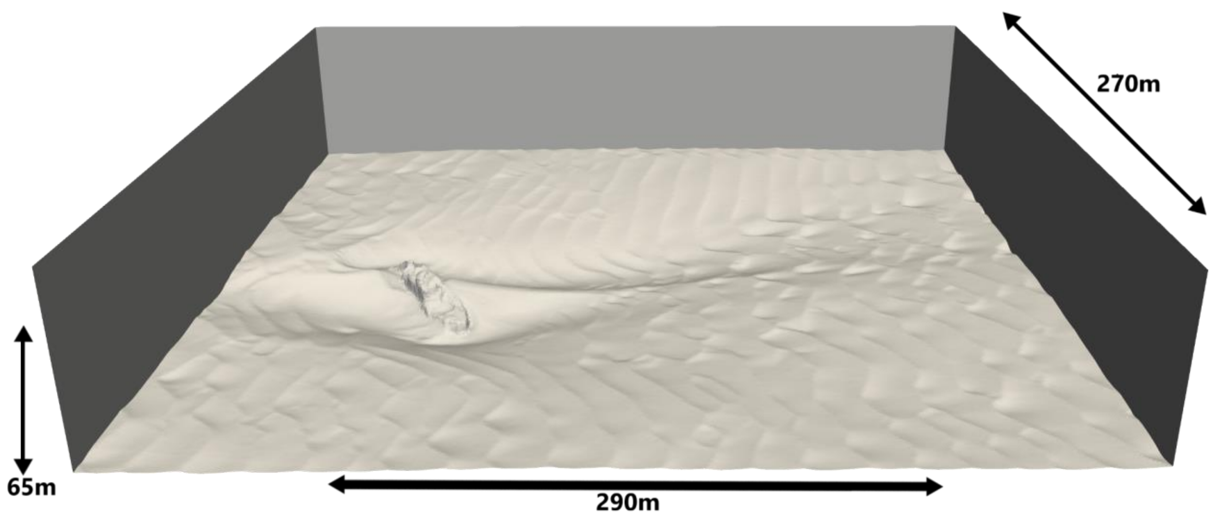

Figure 11. *Computational domain for the SS Hare*

3.6 Computational Mesh

The computational mesh used in the simulations was created using OpenFOAM utilities *blockMesh* and *snappyHexMesh* (Figures 12, 13). It is a hybrid mesh containing a structured background grid and an unstructured hexahedron-dominated mesh in the near-wall region. Guidelines for best practices with CFD are defined by Casey and Wintergerste (2000). Tolias et al. (2019) re-examine these guidelines and suggest several general practices to reduce errors and increase the accuracy and quality of numerical simulations. For the mesh produced by *snappyhexmesh*, a mesh independence study should be performed. This involves starting with a coarse mesh and refining it, with each step having double the cells of the previous. Once the results converge for several mesh densities, the coarsest mesh should be used that still maintains results identical to the finer meshes, to reduce the computational load. Highly skewed cells (for hexahedral cells <40 degrees or >140 degrees) should be avoided due to deterioration in the results (Casey and Wintergerste, 2000).

Best practice guidance on domain size by Franke et al. (2007) suggests the domain should be based on the height and lateral extension of the obstacle involved. Mo et al. (2021) further expand on this for the flow of wind turbines. Although the subjects of these studies differ from the model included in this paper in that they are concerned with the flow of air currents as opposed to water currents, the overarching point remains valid: the domain size is relative to the dimensions of the object of the study. Although Franke et al. (2007) suggests vertical extension at five times the height of the object, our model is defined by the depth of the wrecks. The *SS Polwell* is still relatively intact and has a height of around 5.5 m at roughly 30 m depth, allowing adequate computational space with slightly over the recommended five times vertical extension. The *SS Hare* is also reasonably intact with a 4 m height, representing a 15 times vertical extension. At much greater depths the main concern would be balancing computational power required with an adequate vertical study zone. Mo et al. (2021) concluded that a computational domain size that is not large enough limits the full development of the flow, so having a slightly larger domain than a limited one could be beneficial. This thesis is aimed at examining scour induced by flow around the wreck by highlighting zones of high shear stress. In this study, the area of seabed immediately adjacent to the shipwreck sites was considered due to the fine-scale construction of the simulation domain and constraints on computing capacity in terms of runtime. The two areas most vital to this study were the approach flow and the wake of the two wrecks. Therefore, the extension of the seabed provided by the repeat survey data was deemed adequate for the model.

3.6.1 SS Polwell

Each *blockMesh* cell was assigned a uniform size of 2 m x 1 m x 2 m in all directions, with the geometry positioned at 0 m on the Y axis. *SnappyHexMesh* was used to generate, position, and refine the seabed and shipwreck geometry (Figure 12). The resulting mesh consisted of 264093 cells with 3 layers defined and an expansion ratio of 1.4. The refinement surfaces were set at 1 and 1. This refines cells that intersect a surface. A mesh sensitivity study was performed, using coarser and finer meshes until mesh independence was achieved. The mesh was considered adequate when computational time was reduced to its minimum, while maintaining a suitable level of detail.

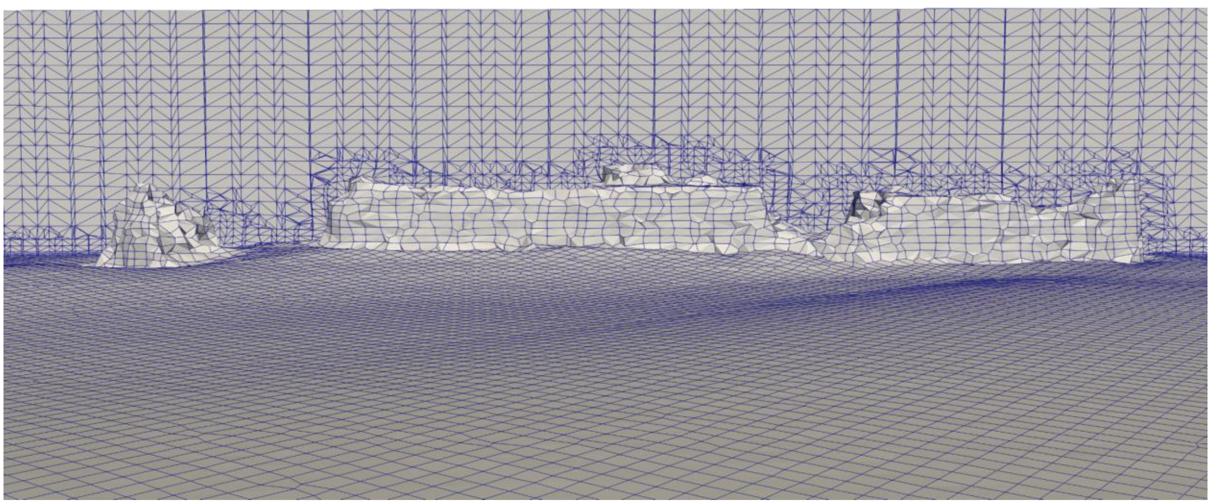

Figure 12. *Computational mesh for the SS Polwell including boundary cells and 3D geometry mesh*

3.6.2 SS Hare

Building upon previous experience with the *SS Polwell*, the computational mesh used for the *SS Hare* was increased in resolution and complexity. In particular, the refinement surfaces were increased to 2 minimum and 2 maximum. The refinement regions were also adjusted to provide a higher level of detail. As with the *SS Polwell*, the domain and geometry meshes used in the simulations were created using OpenFOAM utilities *blockMesh* and *snappyHexMesh* (Figure 13). Cells for the *blockMesh* were assigned a uniform size of 3.5 m x 3 m x 3.2 m in all directions, with the geometry positioned at 0 m on the Y axis. *SnappyHexMesh* was adjusted, based on the previous model with the *SS Polwell*, to provide a higher resolution comparatively. The resulting mesh consisted of 835110 cells with 3 layers defined and an expansion ratio of 1.4. A mesh sensitivity study was also performed to achieve mesh independence, as with the previous model.

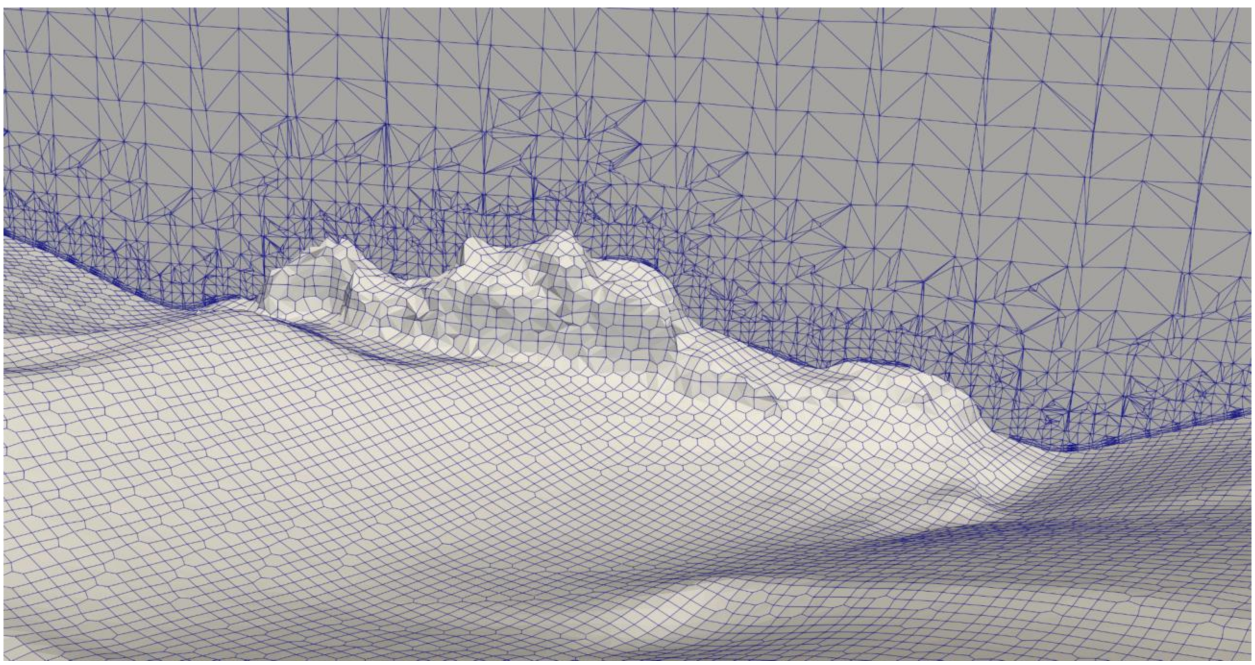

Figure 13. *Computational mesh for the SS Hare including boundary cells and 3D geometry mesh*

4 Results

CFD model outputs for flow velocity, flow patterns and bed shear stress were visualised and analysed in ESRI ArcMap version 10.7 and ParaVIEW version 5.9.0. Analysis was carried out on results from two separate simulations representing the dominant flow directions for the *SS Polwell*: from NW to SE and SE to NW based on the prevailing flow conditions. This process was repeated for the *SS Hare* using the same dominant flow directions with updated parameters according to repeat survey data.

4.1 Flow Velocity and Patterns

4.1.1 SS Polwell

Bed flow velocity values were derived from the cells immediately adjacent to the seabed. Figure 14 shows a maximum velocity value of 0.26 m/s and a minimum value of 0.001 m/s for the NW to SE flow and a maximum of 0.25 m/s and a minimum of 0.006 for the SE to NW flow. The mean current speed for the NE was 0.09 m/s, and 0.08 m/s for the SE.

Flow rates from the NW were divided and categorized as low velocity (0.001-0.07 m/s), medium velocity (0.07-0.12 m/s) and high velocity (>0.12 m/s), based on the Jenks natural breaks classification of the velocity distribution (Chen et al., 2013). The Jenks natural breaks classification method determines the best arrangement of values into different classes by minimizing each class's average deviation from the mean, while maximizing each class's deviation from the means of the other groups. Flow rates for the SE were categorised as low velocity (0.0006-0.06m/s), medium velocity (0.06-0.11 m/s), and high velocity (>0.11 m/s).

Flow from the NW displays a large area of high velocity flow, directly in the central wake of the wreck (Figure 14a). This area is surrounded on either side by a low velocity area, wrapping itself around the wreck's bow and stern, producing a typical wake flow. The flow from the bow appears much more pronounced, flowing through the large break in the hull. Another small area of high velocity flow emerges on the outside of the bow wake, sandwiching the lower velocity flow in between itself and the central wake. As the approach flow makes contact with the wreck on its starboard side it produces two distinct areas of low velocity: at the stern and at the break in the midsection. The areas of high and low velocity are paralleled by a mid-velocity flow on either side.

The high velocities in the flow from the SE to NW (Figure 14b) are concentrated mainly towards the bow of the wreck, pushing through the gap in the bow. The high velocity wake is intersected by a thin stream of low velocity flow and bordered by another to the SW. A large low velocity wake emerges from the stern, separated from the main high velocity wake by a low-mid flow. Again, the approach flow produces areas of low velocity upon reaching the wreck directly, however they span the entirety of the wreck from bow to stern, with a small high velocity area appearing in front of the separated bow section. A medium velocity flow runs either side of the main wake.

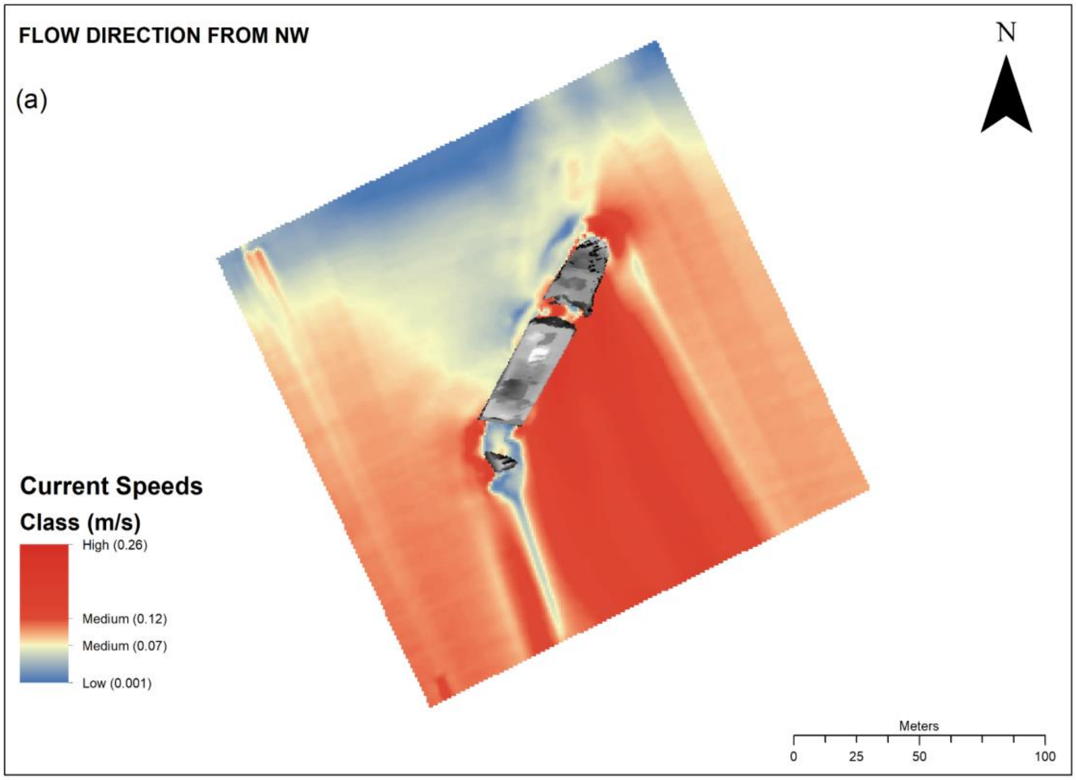

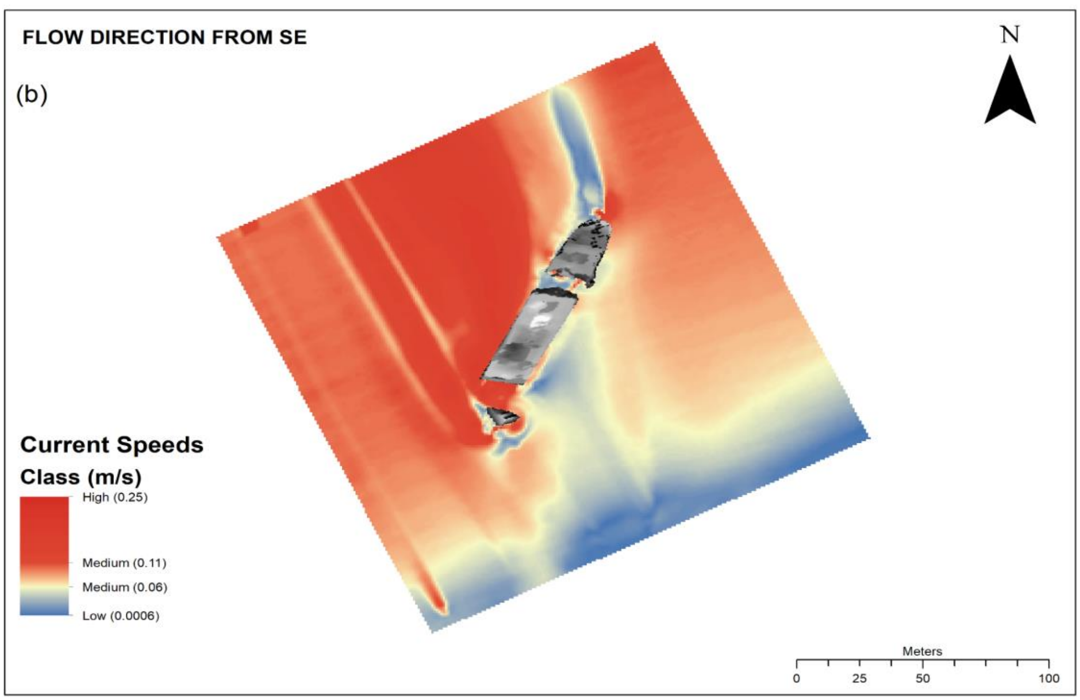

Figure 14. *Maps representing current velocities close to the seabed for flow from the NW (a) and flow from the SE (b)*

Streamline models were generated in ParaVIEW for both current directions (Figure 15), showing more complex flow velocity patterns overlaid on bed shear stress values. Flow velocity for both directions ranged from 0.0047 m/s to 0.22 m/s.

Figure 15a shows the flow from the NW to SE. A mainly laminar flow is prevalent east and west of the wreck, where the flow does not make direct contact and shear stress is minimal. As the flow interacts directly with the wreck however, complex patterns emerge in the wake where horizontal flow separation occurs. As water flows around the wreck's stern, it turns inward towards the wreck where two major low velocity vortices form. These vortices occur where the bed shear stress is highest, losing rotation as they continue towards the outflow of the study area. The break towards the ship's stern appears to be a major contributing factor towards the formation of these vortices.

The SE to NW flow shows a similar pattern of vortices where it interacts with the wreck, with steady, laminar flows either side (Figure 15b). Similarly, it shows the formation of two distinct vortices, through the gap in the hull towards the bow of the ship; the first, towards the east is a significantly developed, low velocity vortex stretching all the way to the stern before being contained by the surrounding flow; the second, towards the west, is a far less developed vortex, distinguished from the surrounding flow by its lower velocity and minimal rotation. Again, where both vortices occur bed shear stress is at its highest.

The seabed signature patterns suggest a degree of symmetry, with noticeable areas of erosion adjacent to the wreck on the west and the east sides. A separate area of deposition occurs to the SE, with a section overlapping the domain. A thin signature of deposition occurs slightly NW of this. Neither of these areas show a symmetrical comparison to the NW to SE flow. The areas of erosion and deposition represented by the repeat survey data compare well with the areas of high and low shear stress generated from the model outputs. In the wreck's wake the boundaries outlining erosional effects follow the model predictions closely, with high shear stress in the centre. The areas outside this high stress area, where velocity and shear stress drop to low values, are outlined by areas of deposition inferred from the repeat survey data. The *SS Polwell* itself is located in an area of deposition predominantly, with the model outputs showing low shear stress in the vicinity of the wreck body.

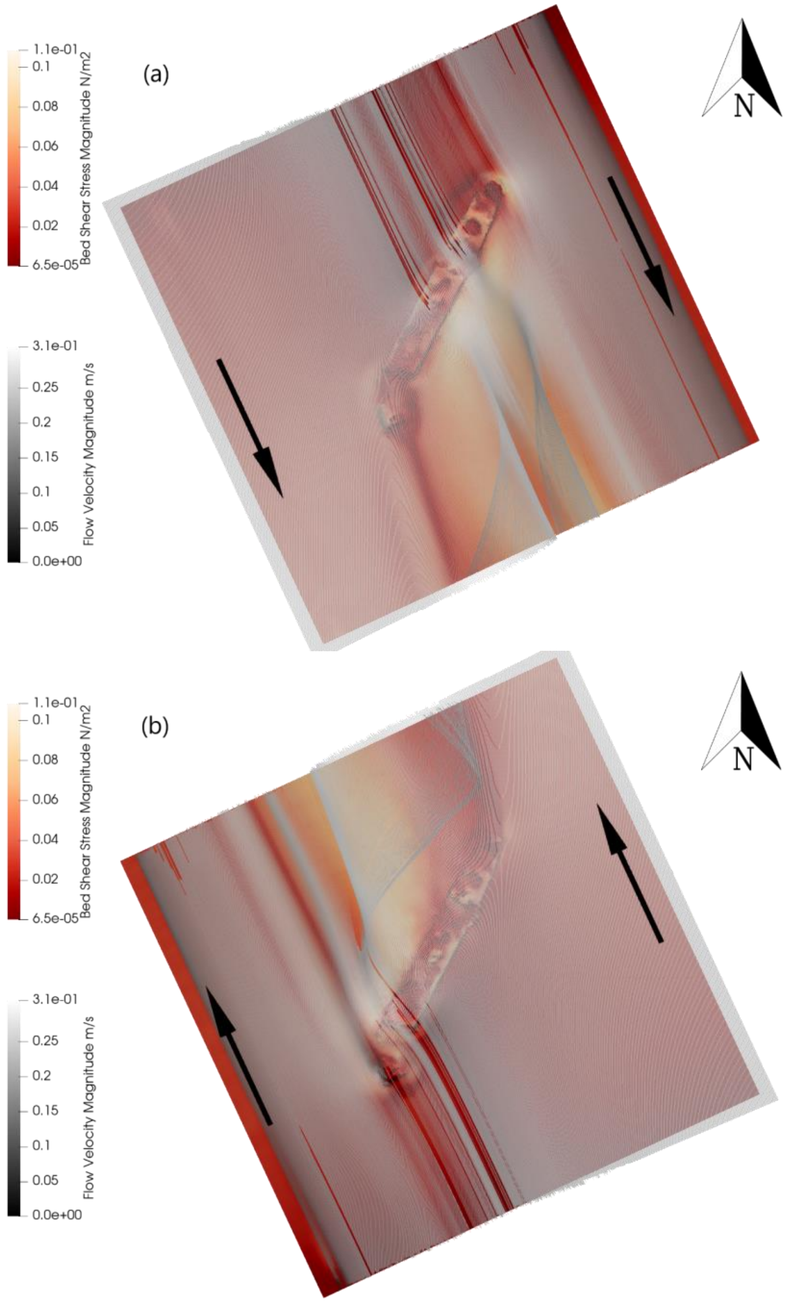

Figure 15. *Streamlines representing current velocity in flow from NW to SE (a) and SE to NW (b)*

4.1.2 SS Hare

Figure 16 shows a maximum velocity value of 0.337 m/s and a minimum value of 0.013 m/s for the NW to SE flow, and a maximum of 0.34 m/s and a minimum of 0.008 m/s for the SE flow. The mean current speed for flow from the NW was 0.134 m/s, and 0.156 m/s for the SE.

Flow rates from the NW were divided and categorized as low velocity (0.013-0.114 m/s), medium velocity (0.114-0.162 m/s) and high velocity (>0.162 m/s). Flow rates for the SE were categorised as low velocity (0.008-0.123 m/s), medium velocity (0.123-0.181 m/s), and high velocity (>0.181 m/s).

The NW to SE flow shows the highest velocities located on the peaks of the sand waves and the top of the wreck (figure 16a). The troughs of the waves display a low or medium velocity where water depth is greater. To the west of the domain is a significant area of almost continuous low velocity, broken where the sand wave peaks are continuous. Flow velocity in the area of the domain to the NW of the wreck exhibits an inconsistent pattern, displaying higher values over the sediment wave crests and lower values in the troughs. This effect lessens in the south of the domain, with more consistent flow speed values and less variance with the bathymetry.

The approach flow directly in front of the wreck shows a large area of low velocity, corresponding with an increase in depth (figure 5). This area contains two sharp lines of low velocity which terminate upon contact with the wreck. South of the wreck lies a large, curved area of high velocity which matches the edge of the large scour pit which the wreck lies in. A band of low velocity lies adjacent to the west of this, corresponding to a ridge of sediment, where water depth decreases.

The SE to NW flow (Figure 16b) shows a less stark variance in terms of the distribution of velocity compared to the simulated flow from the NW, with generally less observed contrast between velocity values between the peaks and troughs of the sand waves. Higher velocity values are still recorded at the peaks of the sediment waves, with lower velocities associated with the wave troughs, although in contrast to the NW dominated flow, they exhibit a more gradual transition from high velocity to low. NW of the wreck, in the western section of the domain, displays the lowest velocity values in the wave troughs.

The area around the wreck is again dominated by low velocity flow. This flow however, has migrated eastwards compared to the NW flow, and shows a very well defined area. It has also extended southwards, towards the approach flow, with an area of medium velocity directly in front of the wreck which wraps around the stern to travel northwards towards the end of the low velocity area.

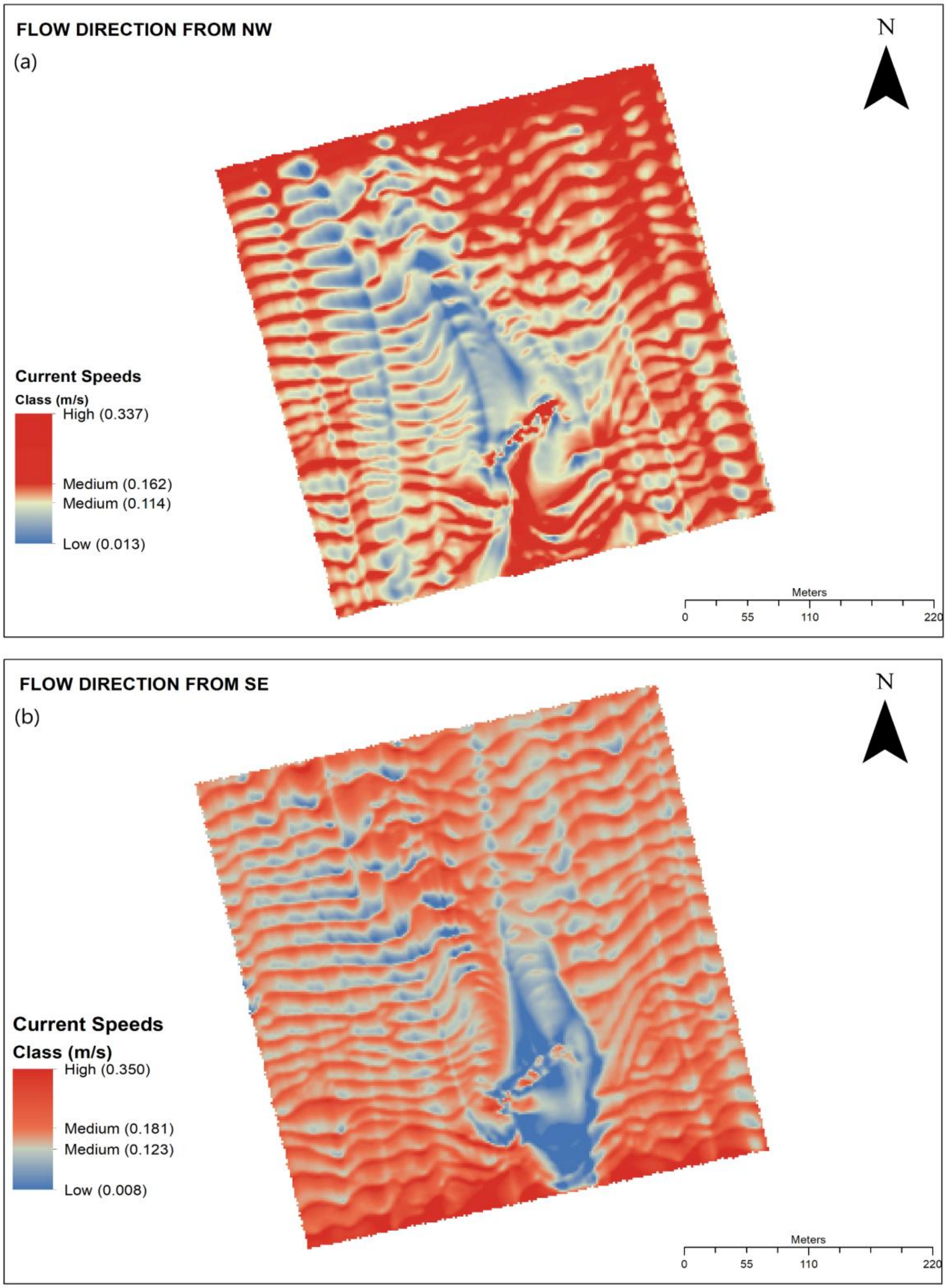

Figure 16. *Maps representing current velocities close to the seabed for flow from the NW (a) and flow from the SE (b)*

Streamline models generated for the NW flow show a generally laminar flow (Figure 17a). Towards the west it can be observed however, that the flow travels slightly inwards towards the centre of the domain, and back outwards as it heads south. This appears to follow and border an area of slightly higher bed shear stress directly west of it. The same effect appears to occur on the opposite side, effectively constricting the flow in the centre.

Where the approach flow contacts the wreck, it curves gently around the bow and stern. From the centre of the wreck to the bow however, the flow twists and forms a clearly defined, high velocity vortex, with the centre flow overlapping the bow flow. This flow correlates with a strip of higher shear stress extending from the wreck to the edge of the domain in the south. There is another area of high shear stress along the stern section of the wreck, where the approach flow makes contact. The areas of highest shear stress across the wider domain correlate with the peaks of the sand waves, with the lowest areas being the troughs in between.

Flow from the SE (Figure 17b) displays the same generally laminar pattern, with a ‘compressed’ area of flow in the centre of the domain. This similarly follows lines from south to north, where higher and lower shear stress meets. There appears to be less definition on these lines compared with the NW dominated flow however, with a gentler curve inward.

The flow around the wreck appears to show a more complex system at work compared to the NW. With the approach flow it can be observed again that it wraps around the bow and stern. Flows over the wreck create multiple vortices that interact. At the stern, the flow over the top shows high velocity, but is undercut by a low velocity vortex. Flow over the centre of the wreck appears to lose velocity somewhat, with lower velocity flow underneath (Figure 17c). The bow of the wreck appears to show significant perturbation of the flow, with spiralling flows of low velocity emerging. As this flow continues north, it continues in a long, thin vortex that gains velocity towards the edge of the domain.

Shear stress across the domain again is most significant where the sand waves peak. Around the wreck however, an area of low shear stress persists for the most part, extending from the approach flow to the wreck, and a similar distance northward. This is interrupted at the bow where the approach flow makes contact, with a small area of high shear stress.

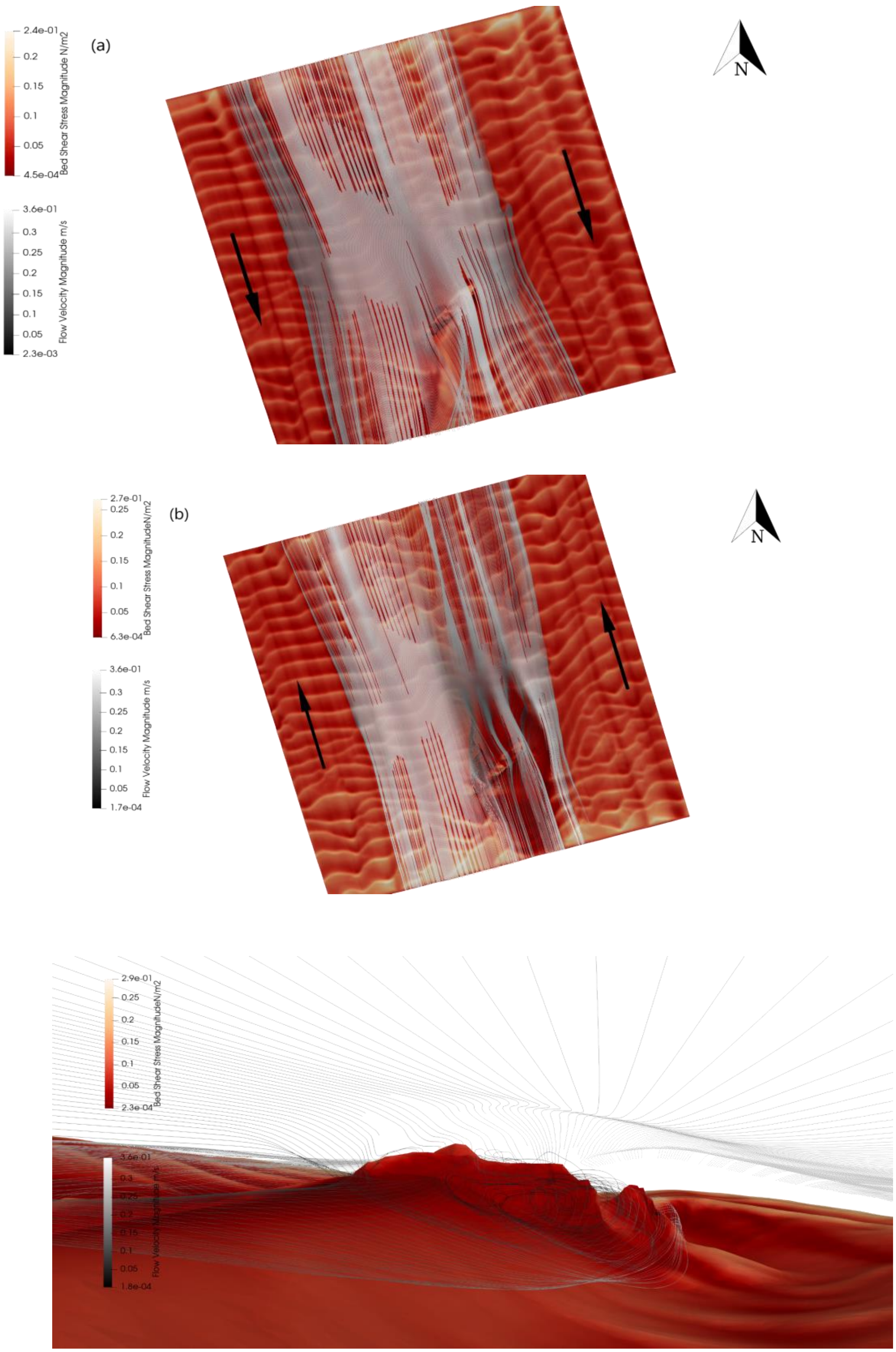

Figure 17. *Streamlines representing current velocity in flow from NW to SE (a), SE to NW (b), detailed view of the wake vortex (c)*

4.2 Validation and Verification

In sediment mobility studies, current speeds are converted to bed shear shear stress to assess the force acting on a particular sediment type (e.g. Whitehouse, 1998). In OpenFOAM, the bed (or wall) shear stress vector (τ_c) is calculated using the built-in *wallShearStress* function at selected wall patches using the equation $\tau c = R \cdot n,$ where R is shear-stress symmetric tensor retrieved from the turbulence model and n is the patch normal vector (into the domain). The resulting values were given in m^2/s^2. By using the calculator function within ParaVIEW, the wall shear stress values were multiplied by the fluid density (seawater at 10 °C, 1027 kg/m^3) in order to give values in Pascals.

4.2.1 SS Polwell Site Sediment Dynamics

Figure 18 shows bed shear stress overlaid with areas exhibiting erosional and depositional signatures defined from survey data by Majcher et al. (2021). The flow originating from the NW displays a maximum value of 0.091Pa and a minimum of 0.00008Pa, with a mean of 0.03Pa (Figure 18a). Flow from the SE displays a maximum value of 0.085Pa and a minimum of 0.00008Pa, with a mean of 0.026Pa (Figure 18b). Both flow directions were also characterized separately as having areas of high, medium, and low shear stress based on natural breaks in the data distribution. Flow rates for the NW were categorised as low shear stress (0.00008-0.02Pa), medium shear stress (0.02-0.04Pa), and high shear stress (>0.04Pa). Flow rates for the SE were categorised as low shear stress (0.00008-0.02Pa), medium shear stress (0.02-0.05Pa), and high shear stress (>0.05Pa). Erosional and depositional signatures defined by Majcher et al., (2021) are based upon time-lapse repeat survey data to provide a comparison with simulated conditions.

Flow from the NW displays a large area of high shear stress in the centre of the wreck's wake, surrounded on either side by areas of low stress. Another, thin area of high stress wraps around the highly defined low stress emerging from the wake of the wreck's bow. There is a small area of high stress in the midship break and a prominent one at the point of the wreck's stern. A large area of low stress is present in the approach flow, making contact with the full length of the wreck. Areas of medium stress are present on either side of the wake.

Flow from the SE displays a large area of high stress in the wreck's wake, skewed towards the bow. Two thin lines of low stress emerge on the SW side of the high stress; one intersecting an area of medium-high stress; the other bordering it. A large, well-defined area of low stress emerges from the stern wake, with a very small area of high stress at the point of the stern and a slightly larger one in the gap between the bow and the main section. As with the NE flow, the approach flow contains a large, low stress area that makes contact along the length of the wreck.

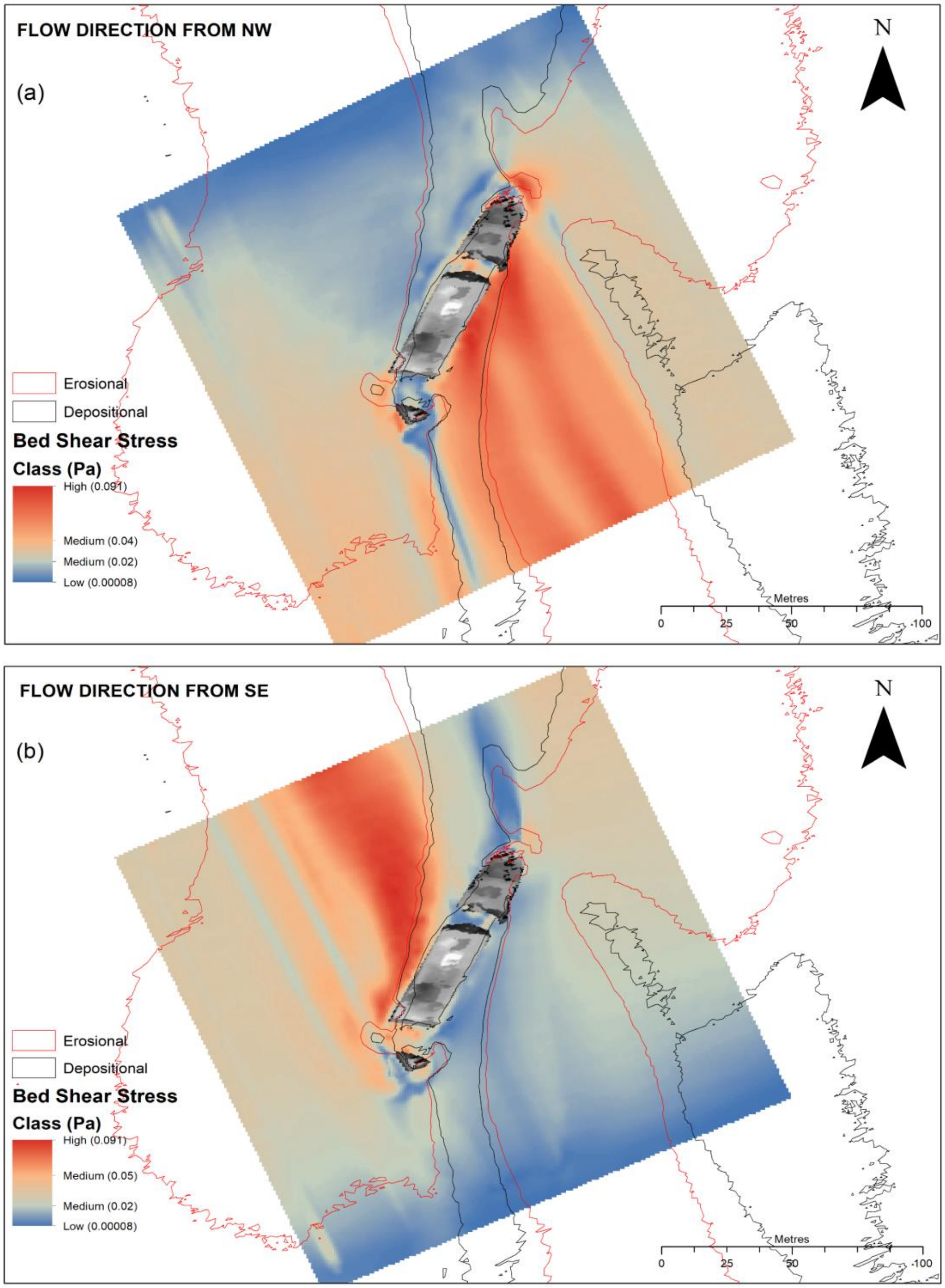

Figure 18. *Maps representing bed shear stress with flow from the NW (a) and flow from the SE (b). Red and black lines represent areas of erosion and deposition*

4.2.2 SS Hare Site Sediment Dynamics

The NW to SE flow shows an area of deposition in the approach flow to the wreck, stretching around 100 m northward (Figure 19a). This coincides with the lower bathymetry where the wreck lies and stretches across the large area of low shear stress. Another, smaller area of deposition lies on the south side of the wreck, where the other side of the depression terminates. It coincides with the area of high velocity observed on the south section of the depression and is intersected by the erosion boundary line.

Outside the largest area of deposition is a larger area of erosion which extends in all directions, but is most extensive to the NW. This covers just outside the large seabed depression and corresponds with the shallower water depths. The wreck itself rests in an area of erosion also, splitting the two areas of deposition.

The SE to NW flow (Figure 19b) displays a much less defined picture deposition when compared to the NW flow. The deposition still coincides with the seabed depression but the large area of deposition north of the wreck crosses high and low shear stress areas. The southern area of deposition lies mostly in an area of low shear stress however. The large area of erosion surrounding the area aligns with the peaks of the sand waves in the area. Similar to the NW to SE flow, the wreck lies inside an erosional signature, but with a less continuous pattern of high shear stress.

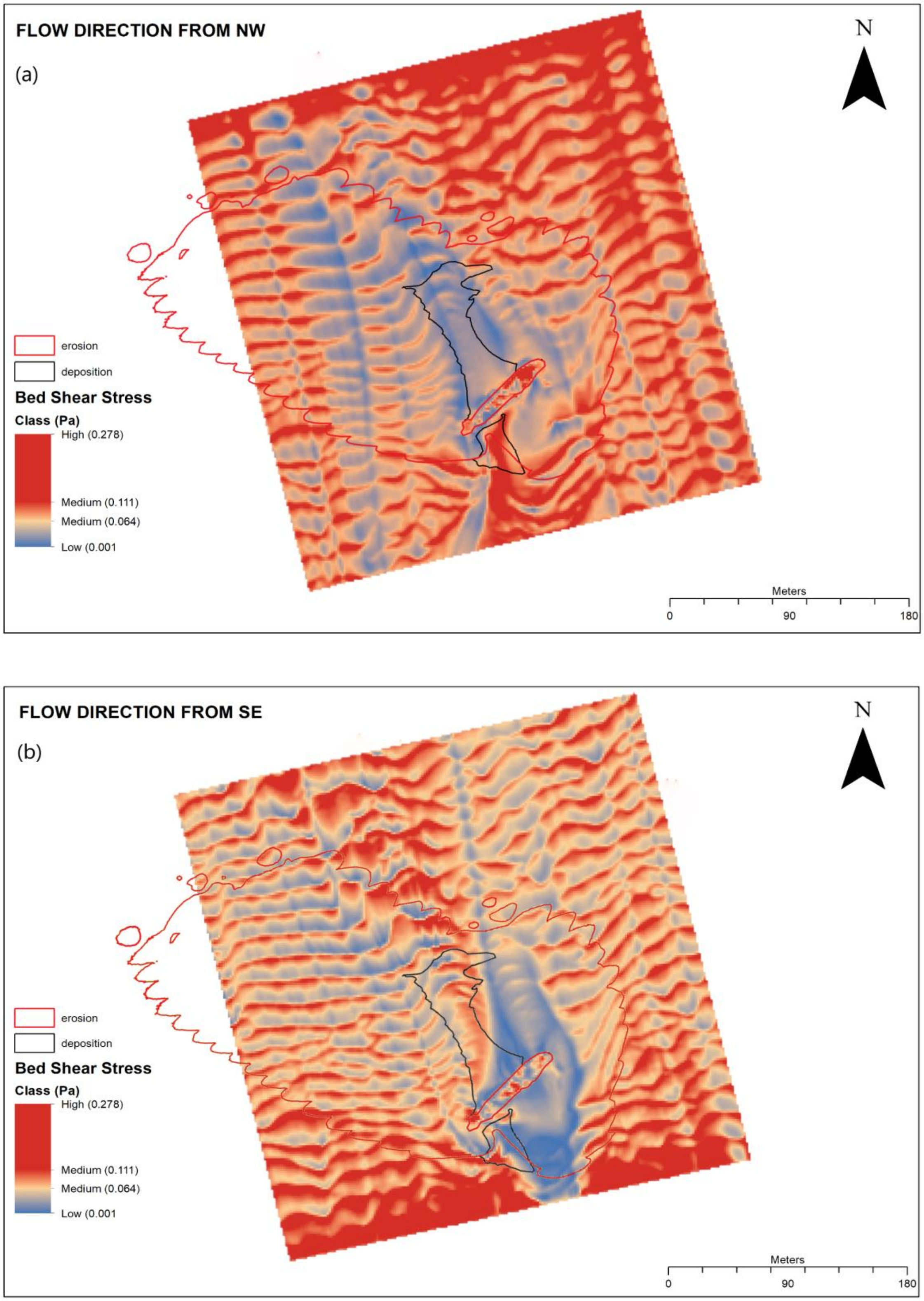

Figure 19 *Maps representing bed shear stress with flow from the NW (a) and flow from the SE (b). Red and black lines represent areas of erosion and deposition*

5 Discussion

5.1 Site and Wreck Comparison

The CFD models appear to show a consistent pattern for flow velocity, behaviour, and bed shear stress. The *SS Polwell* displays a typical flow pattern in its wake, created by pressure gradients due to the flow around and over the wreck (Quinn and Smyth, 2018), as does the *SS Hare*. The flow in the direct wake of the wrecks shows an exception, however. In this case, the velocity drops in the immediate vicinity, gaining velocity again as it travels towards the edge of the domain, yet it still correlates with high shear stress. This is probably due to the complex and turbulent nature of the flow and while it loses some straight-line velocity, the flow's energy is instead concentrated on a fixed area. This is reflected in the amplification factor for shear stress, with both wrecks showing an increase by a factor of around four in the wreck's wake, compared to the ambient shear stress in the general areas. This amplification of shear stress agrees with findings by Smyth and Quinn (2014) and Whitehouse (1998), where they highlight that shear stress is amplified by an obstacle's presence by a factor of three to four.

The overall bathymetry differs greatly between the two wrecks. The *SS Polwell* lies in an area almost entirely devoid of recognisable bedforms. This is due to the difference in velocity observed at both sites. The *Polwell* experiences lower current velocities in its area in general. The velocity profile based on the mean depth-averaged velocity of 0.147 m/s suggests that there is less energy in the overall area's flow compared with the *SS Hare*, meaning sediment outside the wreck's direct vicinity could be subject to less mobilisation as there are no obstacles to provide an amplification factor. The multimodal nature of the sediment in the area (gravelly, muddy sand) contributes to the lack of bedform features with the lower energy flow unable to mobilise the coarser sediment. Temporal comparison of repeat survey data shows that the area does not show signs of significant scour, instead suggesting a slight tendency toward deposition (Majcher et al., 2020). The area around the *SS Hare* is dominated by sand waves across the entire domain. Unlike the *Polwell*, the *Hare* lies in an area composed mostly of sand with a higher mean depth-averaged velocity of 0.23m/s providing the basis for the velocity profile. This, combined with a monomodal, less coarse sediment type (i.e. sand) enables the transport of larger volumes of sediment

The overall depth range for the domain of the *SS Polwell* is around 10 m from the deepest to the shallowest areas (Figure 4). The *SS Hare* however, lies in an area with roughly a 21 m depth range (Figure 5), mostly due to the scour pit created by the presence of the wreck increasing the depth compared to the ambient seabed. This scour pit demonstrates that the factors such as velocity and sediment type can have a great impact on scour created by obstacles on the seabed. The fact that the CFD model shows a lack of shear stress in the area now suggests that it may have reached its equilibrium depth, with little or no further scour occurring. The *SS Polwell's* tendency toward deposition in close proximity to the wreck, along with higher shear stresses in these areas, suggests a recycling of sediment caused by the turbulent vortices in the wreck's wake. While capable of sediment transport, these vortices lack the velocity and energy in the wider area, instead depositing the suspended sediment close to the wreck. This sediment is then mobilised upon the switch in current between NW and SE and deposited in the same way towards the wreck, creating a mock-closed sediment budget, with very little transported in from outside the immediate area.

5.2 CFD Model Simulation Methodology

Although the same general parameters (e.g. boundary type) were used for both shipwrecks, as the seabed and current conditions were unique to each there were subtle differences in the CFD modelling methodology that are worth discussing.

In order to understand seabed hydrodynamics, previous studies have employed the use of repeat surveys and *in-situ* monitoring devices (Bauri and Sarkar 2016; Majcher et al., 2020). The results from this study suggest that CFD modelling is capable of producing outputs that can be validated by real-world survey data, in order to explain the complex interactions of seabed hydrodynamics. By examining a summation of survey data, velocity values, shear stress, and flow regimes we have created a multidimensional, multipurpose model.

Both models were tested at several mesh resolutions in snappyhexmesh in order to balance computational load with a high level of detail, with the *SS Hare* building upon the methods employed when modelling the *SS Polwell*. In both cases, *snappyhexmesh* was started at a high level of detail, using a very fine mesh, and lowered gradually until a balance between detail and computational effort was achieved (mesh independence). Both were ultimately limited in detail by the 3-D .stl files, both of which contained small data gaps that were invisible upon initial inspection, but became exposed upon increasing the resolution of snappyhexmesh past certain thresholds unique to each model and flow direction. This resulted in greatly exaggerated values for all parameters upon running the model, as the fluid was forced through these holes, causing the model to fail. In relation to the best practice guidelines for vertical extension of the domain in relation to the obstacle height, the *SS Hare* was given its full 60 m depth in order to correctly represent the velocity profile, and limit the possible effects and errors introduced by reducing the vertical domain and profile values.

In both of the streamline flow models for the *SS Hare*, a constriction of the flowlines in the centre of the domain is observed in the results. This could be an effect of the domain size as there appear to be no observable influencing factors such as bathymetric changes or bedforms. It is more likely however, that it is an effect of the scour pit as the flow in the CFD model traverses it and no similar effects have been observed with the *SS Polwell*, which shows no scour pits or significant changes in bathymetry.

The initial boundary conditions applied to the model were chosen based on previous work by Quinn and Smyth (2018). The 'front' and 'back' of the domain were designated as 'symmetry' boundary types to provide zero interference with the flow while establishing a boundary for calculations. Other types of boundary could potentially act as a solid restriction, interfering with the flow and causing unwanted noise. Initially, the mean depth-averaged velocity was used as an input to the *SS Polwell's* inlet boundary. It was recognised that this did not accurately represent the effect of friction at the seabed acting on the flow, in addition to the fact that the depth-averaged velocity readings were taken in the water column, and not at the seabed itself. Therefore, a velocity profile based on the mean depth-averaged velocity was applied at both wreck's inlets, representing the dynamic nature of current velocity throughout the water column.

5.3 Limitations and further work

In taking a 'snapshot' of the area directly around the wreck we limit the development of the flow in approaching the obstacle in addition to the effects after contact with it. To the north of the *SS Polwell*, for example, lies a pipeline (Figure 4) in a roughly east to west orientation which could perturb the approach flow from the NW before it reaches the wreck. To the south is an area of complex bedforms which could serve to complicate the approach flow from the SE. In order to correct for this, the area included in the model could be expanded to include a wider view. This would require vast amounts of computing power however, and even using UCD's Sonic Cluster, this could take weeks to complete, making it impractical. Another option could be to model both of these areas separately and feed the output from these models into a newer, high-resolution model concentrating solely on the wreck and its immediate surroundings. Again, this would involve increased computational effort, but the two ‘approach’ sections could be modelled in parallel saving time.

For the purposes of this study the steady-state solver SimpleFOAM was employed as this study was focused specifically on verification and validation of a CFD model using data for both wrecks taken from the survey between the 4th and the 10th of October 2019 (CV19027). However, seabed sediment dynamics, and in particular scour development, can evolve significantly over time and so require transient solvers (Quinn and Smyth, 2018; Smyth and Quinn, 2014). At the shipwreck sites there is repeat bathymetric survey data that would allow for assessment of geomorphic change over varying temporal timescales ranging from 1-week to 1-year to 4-years (the *Polwell* was surveyed in 2015, 2016 and 2019, the *Hare* shares these dates but was surveyed in 2010 also. Detailed analysis of these temporal changes would require a large-scale transient solver such as PimpleFOAM in order to provide an in-depth analysis of scour evolution over time.

The multimodal nature of sediment at the seafloor of the *SS Polwe*ll site represents a complex geological setting in terms of sediment distribution (Figure 4). As a result, no single value for the threshold of movement can be applied to the site to determine sediment mobility, making it difficult to calculate net movement of sediment and precise levels of scour or deposition. The mobilisation of the sediment particles is governed by the Shields parameter:

$$\boldsymbol{\tau}^* = \boldsymbol{\tau}/(\rho s - \rho)gD' \quad (2)$$

where:

- $\boldsymbol{\tau}$ is the dimensional shear stress;
- ρs is sediment density;
- ρ is the fluid density;
- g is the gravitational acceleration;
- D is the particle diameter of the sediment.

Pang et al. (2016) demonstrated a critical Shields value that corresponds with the equilibrium scour depth. Majcher et al. (2021) utilised regionally modelled current speed data from the Marine Institute ROMS-based model to calculate exceedance values for sediment types at differing shipwreck sites. As highlighted in this study, values for bed shear stress across sites with an obstacle (i.e. a shipwreck) can vary considerably depending on amplification factors associated with that obstacle, as well as seabed morphology. In this instance, shear stress values were increased by a factor of around 4 in the immediate vicinity of both wrecks. Using more detailed current speed (i.e. and calculated bed-stress data outputs from the model developed in this study, in conjunction with a sediment grain-size database, would allow for a much more robust assessment of sediment mobility due to threshold exceedance. Application of a sediment transport model such as that used by Jacobson and Fredsoe (2014) could also serve to elucidate sediment specific behaviour under shear stress when combined with a CFD model.

The Integrated Mapping for the Sustainable Development of Ireland's Marine Resource (INFOMAR) programme has been mapping the Irish seabed since 2006, and in that time has mapped some 457 shipwrecks in varying degrees of detail. The quality of this database, and it's broad geographic extent, means that the approach described here can be applied to a significant number of other sites in the Irish territory in differing hydrodynamic and seabed morphological and sedimentary settings. A future examination of multiple seabed obstructions and/or morphology types and their effects on the overall flow regime in this manner could serve to elucidate the complex nature of obstacle induced hydrodynamic flow and scour development, allowing for an extensive, regional assessment of scour potential.

Further work could involve reinforcing the results of the CFD model by including lab-based testing with an experimental flume. 3D printing could provide scaled-down 'monopiles' and other structures to place in the flume, placing them in different sediment types, observing scour patterns, and comparing them with results from CFD cases. Additionally, the CFD models, while highly accurate and cost-effective, are time intensive and adaptation to new inputs can be complicated. With advancements in physics based A.I. learning, a model based on this CFD technique could be developed that is adaptable to varying conditions and inputs, reduces potential human error, and requires far less computational effort and time.

6 Conclusions

The aim of this thesis was to build upon existing literature using CFD to model current flow patterns and scour potential around seabed structures, using shipwrecks as proxies. This was to provide an effective and state-of-the-art de-risking tool for renewable energy planning in the offshore environment. Currently, there is a significant knowledge gap as to how and when scour will occur, with no single tool or method able to account for the complex mix of conditions on the seabed. This approach addresses the gap and provides a means by which to model the scour potential around seabed infrastructure. This method can address some of the issues with marine spatial planning and help to reach goals set out in Ireland's Climate Action and Low Carbon Development Bill, furthering the steps towards carbon neutrality of Ireland's energy production.

Two shipwrecks were chosen as case studies: the SS Polwell and the SS Hare. The former laid in a low current speed section of the seabed, with signs of deposition shown from repeat survey data. The latter rests in an area of higher current speed, within a large scour hole. The CFD software OpenFOAM was used to create numerical models which simulate current flow through a predesignated domain, in order to measure current velocity, behaviour, and bed shear stress around the wreck. The SS Polwell was found to be in an area favouring deposition, with the highest areas of shear stress correlating with vortices in the wreck's wake, where deposition was dominant, due to the flow quickly losing energy as it rose from the seabed. The model for the SS Hare showed it was in an area of higher shear stress, compared with the Polwell. The area itself was full of bedforms, suggesting the transport of sediment was taking place. Vortices from the wreck's wake were elongated and retained much more velocity than the Polwell. The findings of these models correlated well with signatures for sediment erosion and deposition from repeat survey data for both wrecks, providing effective validation of the method.

When applied to the hydrodynamic regime governing seabed interactions, CFD provides a novel, high-resolution approach. This model can be combined with detailed bathymetric data to provide a robust and accurate overview of fluid flow and its effect on scour. Repeat and physical (i.e. grab sample) data can be used in conjunction with the outputs from this model in order to elucidate localised temporal sediment dynamics and morphological change. This approach can be applied and adapted to other artificial structures such as offshore wind turbine foundations, or pipelines, and serve to de-risk seabed infrastructure planning.

By further developing this method and streamlining the process, an efficient model can be developed to inform the planning phase of such structures with a view to protect from instability, or protection of important archaeological sites or habitats.

References

Bauri, K.P. and Sarkar, A., 2016. Flow and scour around vertical submerged structures. *Sādhanā*, *41*(9), pp.1039-1053.

Calder, B. and Wells, D.E., 2007. CUBE user's manual. Durham: University of New Hampshire. http://ccom.unh.edu/sites/default/files/publications/Calder_07_CUBE_User_Manual.pdf

Casey, M. and Wintergerste, T., 2000. *Best practice guidelines*. [S.l.]: ERCOFTAC.

Chen, J., Yang, S., Li, H., Zhang, B. and Lv, J., 2013. Research on Geographical Environment Unit Division Based on the Method of Natural Breaks (Jenks). *The International Archives of the Photogrammetry, Remote Sensing and Spatial Information Sciences*, XL-4/W3, pp.47-50.

Fernández-Montblanc, T., Izquierdo, A., Quinn, R. and Bethencourt, M., 2018. Waves and wrecks: A computational fluid dynamic study in an underwater archaeological site. *Ocean Engineering*, 163, pp.232-250.

Franke, J., Hellsten, A., Schlunzen, K.H. and Carissimo, B., 2011. The COST 732 Best Practice Guideline for CFD simulation of flows in the urban environment: a summary. *International Journal of Environment and Pollution*, *44*(1-4), pp.419-427.

Gatzert, N. and Kosub, T., 2016. Risks and risk management of renewable energy projects: The case of onshore and offshore wind parks. *Renewable and Sustainable Energy Reviews*, 60, pp.982-998.

Li, Y., Ong, M.C., Fuhrman, D.R. and Larsen, B.E., 2020. Numerical investigation of wave-plus-current induced scour beneath two submarine pipelines in tandem. *Coastal Engineering*, *156*, p.103619.

Lewis, M., Neill, S., Robins, P., Hashemi, M. and Ward, S., 2017. Characteristics of the velocity profile at tidal-stream energy sites. *Renewable Energy*, 114, pp.258-272.

Ma, H. and Chen, C., 2021. Scour protection assessment of monopile foundation design for offshore wind turbines. *Ocean Engineering*, *231*, p.109083.

Majcher, J., Plets, R. and Quinn, R., 2020. Residual relief modelling: Digital elevation enhancement for shipwreck site characterisation. *Archaeological and Anthropological Sciences*, *12*, pp.1-13.

Majcher, J., Quinn, R., Plets, R., Coughlan, M., McGonigle, C., Sacchetti, F. and Westley, K., 2021. Spatial and temporal variability in geomorphic change at tidally influenced shipwreck sites: The use of time-lapse multibeam data for the assessment of site formation processes. *Geoarchaeology*, *36*(3), pp.429-454.

Matutano, C., Negro, V., López-Gutiérrez, J.S. and Esteban, M.D., 2013. Scour prediction and scour protections in offshore wind farms. *Renewable energy*, *57*, pp.358-365.

Mellet, C., Long, D., Carter, G., Chiverrell, R., Van Landeghem, K., 2015. Geology of the seabed and shallow subsurface: The Irish Sea. *British Geological Survey Commissioned Report, CR/15/057.* 52pp.

Mo, J.O., Choudhry, A., Arjomandi, M., Kelso, R. and Lee, Y.H., 2013. Effects of wind speed changes on wake instability of a wind turbine in a virtual wind tunnel using large eddy simulation. *Journal of Wind Engineering and Industrial Aerodynamics*, *117*, pp.38-56.

Nagy, H., Lyons, K., Nolan, G., Cure, M., & Dabrowski, T. 2020. A Regional Operational Model for the North East Atlantic: Model Configuration and Validation. *Journal of Marine Science and Engineering,* Vol. 8, Issue 9. https://doi.org/10.3390/jmse8090673

Pang, A.L.J., Skote, M., Lim, S.Y., Gullman-Strand, J. and Morgan, N., 2016. A numerical approach for determining equilibrium scour depth around a mono-pile due to steady currents. *Applied Ocean Research*, *57*, pp.114-124.

Quinn, R., Bull, J. and Dix, J., 1997. Buried scour marks as indicators of palaeo-current direction at the Mary Rose wreck site. *Marine Geology*, 140(3-4), pp.405-413.

Quinn, R. and Smyth, T.A.G., 2018. Processes and patterns of flow, erosion, and deposition at shipwreck sites: a computational fluid dynamic simulation. *Archaeological and Anthropological Sciences*, *10*(6), pp.1429-1442.

Schendel, A., 2018. *Wave-current-induced scouring processes and protection by widely graded material* (Doctoral dissertation, Hannover: Institutionelles Repositorium der Leibniz Universität Hannover).

Shchepetkin, A.F. and McWilliams, J.C., 2005. The regional oceanic modeling system (ROMS): a split-explicit, free-surface, topography-following-coordinate oceanic model. *Ocean modelling*, *9*(4), pp.347-404.

Smyth, T. and Quinn, R., 2014. The role of computational fluid dynamics in understanding shipwreck site formation processes. *Journal of Archaeological Science*, 45, pp.220-225.

Soulsby, R., 2017. *Dynamics of marine sands*. London: Thomas Telford.

Tolias, I., Giannissi, S., Venetsanos, A., Keenan, J., Shentsov, V., Makarov, D., Coldrick, S., Kotchourko, A., Ren, K., Jedicke, O., Melideo, D., Baraldi, D., Slater, S., Duclos, A., Verbecke, F. and Molkov, V., 2019. Best practice guidelines in numerical simulations and CFD benchmarking for hydrogen safety applications. *International Journal of Hydrogen Energy*, 44(17), pp.9050-9062.

De Vos, L., De Rouck, J., Troch, P. and Frigaard, P., 2011. Empirical design of scour protections around monopile foundations: Part 1: Static approach. *Coastal Engineering*, *58*(6), pp.540-553.

De Vos, L., De Rouck, J., Troch, P. and Frigaard, P., 2012. Empirical design of scour protections around monopile foundations. Part 2: Dynamic approach. *Coastal Engineering*, *60*, pp.286-298.

Welzel, M., Schendel, A., Hildebrandt, A. and Schlurmann, T., 2019. Scour development around a jacket structure in combined waves and current conditions compared to monopile foundations. *Coastal Engineering*, *152*, p.103515.

Westley, K., Plets, R., Quinn, R., McGonigle, C., Sacchetti, F., Dale, M., McNeary, R., & Clements, A. 2019. Optimising protocols for high-definition imaging of historic shipwrecks using multibeam echosounder. *Archaeological and Anthropological Sciences*, 3629–3645. https://doi.org/10.1007/s12520-019-00831-6

Whitehouse, R., 1998. *Scour at marine structures*. London: Thomas Telford Ltd.

Whitehouse, R.J., Sutherland, J. and Harris, J.M., 2011, December. Evaluating scour at marine gravity foundations. In *Proceedings of the Institution of Civil Engineers-Maritime Engineering* (Vol. 164, No. 4, pp. 143-157). Thomas Telford Ltd.

Yang, B., Wei, K., Yang, W., Li, T. and Qin, B., 2021. A feasibility study of reducing scour around monopile foundation using a tidal current turbine. *Ocean Engineering*, *220*, p.108396.

Understanding sediment dynamics at a shipwreck site using CFD modelling

Authors: Gary Littler, Mark Coughlan, Jan Majcher, Jennifer Keenahan

Abstract

Seabed hydrodynamics and sediment mobility pose significant threats to offshore engineering infrastructure, not least of all renewable energy installations such as turbine monopile foundations. Such infrastructure can introduce seafloor obstacles that perturb the local environment inducing scour that can cause structural instability, or deposition resulting in the burying of infrastructure. Understanding the processes that drive these complex patterns of sediment erosion and deposition over varying timescales is critical to the sustainable development of critical offshore infrastructure. Traditionally assessments for such issues have utilised time-lapse bathymetric surveys and scaled physical testing. The former fails to capture the nuance of these processes between data collection surveys and cannot predict how the seabed will react to an obstacle, whilst the latter is costly and limited in recreating the marine environment. Computational Fluid Dynamics (CFD) modelling however, offers an effective means of investigating the complex interaction between hydrodynamics and manmade objects on the seafloor. Similarly, shipwrecks offer natural laboratories with which to validate models using CFD approaches. In this study, CFD simulations are generated for a high-resolution bathymetric survey dataset of a shipwreck site and assessed for application in future scour prediction studies.

1. Introduction

Shipwrecks on the seabed are generally avoided in terms of offshore wind development as they are protected locations of high cultural heritage value. However, increasingly they are being used as natural laboratories on the seabed to study the complex interaction of man-made objects, seafloor sediment transport and hydrodynamic processes (Majcher et al., 2021). Offshore wind is seen as a critical technology towards decarbonising electricity demand. When it comes to siting individual turbines on the seafloor, the issue of seabed mobility and the potential for scour development is a significant geohazard and environmental constraint associated with the development of this sector, as well as other engineering infrastructure such as pipelines and cables (Mellet et al., 2015). Scour is the process in which sediment is eroded and transported due to an imposed shear stress generated by seabed current and/or waves. Its effects have been widely reported, documented and examined (Quinn, Bull and Dix, 1997); Bauri and Sarkar 2016; Schendel et al., 2018). The rate of erosion is largely dependent on the energy generated by local flow regimes and the properties of the sediment at the seafloor.

Whilst scour is a naturally occurring phenomenon, the introduction of obstacles into a system can magnify the effects due to an increase in bed shear stress caused by fluid flowing around the obstacle creating pressure differences, increased flow velocity and turbulence. Over time this can lead to the formation of scour holes around the obstacle where the shear stress is highest, and deposition as the energy and turbidity of the flow decreases to the point the suspended sediment can no longer be transported in the water column. These scour holes can lead to damage and destabilisation of structures such as turbine foundations and "free-spanning" of cables, requiring concerted efforts to remediate existing damage and prevent further scour occuring. Mitigating defences such as rock armour can be utilised after initial installation, and have been extensively examined (Vos et al., 2011, 2012; Ma and Chen, 2021). These can be technically difficult to implement however, making them financially costly when installed after scour has occurred or placed in anticipation of possible issues. Ireland's only offshore wind farm constructed to date, Arklow Bank, experienced scour issues that had a significant impact on the project resulting in the use of rock armour in an attempt to mitigate against further scour and turbine instability (Whitehouse et al., 2011). Therefore, pre-empting such issues and Identifying the optimum area for placement of defences, or avoiding areas of high shear stress altogether, can increase the viability and longevity of installations. Based on experiences across Europe, there is a significant amount of focus on geotechnical assessments for scour and related processes in relation to offshore engineering and mitigation (Matutano et al. 2013). Efforts to predict sediment dynamics and scour evolution can be challenging, as *in-situ* measurements and observations involve using remote sensing techniques with visual interpretation of the seabed features (Quinn, Bull and Dix, 1997) without examining current flow dynamics. These methods can be costly, time-consuming, and provide an incomplete understanding of the forces at work due to the large scale of the task. Other methods include small laboratory-based modelling (Schendel et al., 2018), larger models contained in specialised facilities (Welzel et al., 2019) or specialized full scale experiments such that performed by Ma and Chen (2021) on the National Renewable Energy Laboratory (NREL) wind turbine in the U.S. There are, however, significant limitations imposed on these methods. Scaling down models introduces unavoidable errors due to the loss of real world variables. Full scale test models still suffer from difficulty recording measurements, although to a lesser extent than their real world counterparts, and conditions such as the weather can hinder prospective studies. In general, there is a clear need for a better understanding of localised seabed dynamics and subsequent impacts on morphodynamics and scour development. However, there is a paucity of direct observations and data on scour development processes.

Computational Fluid Dynamics (CFD) is a tool that can be used to model a section of the seabed, along with any obstacles within with respect to current flow dynamics. Therefore, the application of CFD modelling is further enhancing the understanding of hydrodynamic processes driving sediment transport and scour (Li, Ong and Fuhrman, 2020). Using a solver based on Navier-Stokes equations, fluid flow can be simulated and its interaction with obstacles analysed. Smyth and Quinn (2014), Quinn and Smyth (2017), Fernández-Montblanc et al., (2018) demonstrated how CFD modelling applied over a shipwreck site could garner significant insight into the hydrodynamic regime, including interaction with seafloor sediments, in understanding scour signature formation processes. When combined with repeat hydrographic surveys that provide high-resolution bathymetric data detailing seabed geomorphic change, CFD is a powerful tool to elucidate patterns of turbulent flow and enhanced currents around seabed obstructions at a localised scale. Turbulence models can also be utilised to increase the accuracy of the model in complex systems, allowing for more detailed analyses of the flow. By using an approach based on CFD it is possible to produce an accurate and cost-effective prediction model for scour on a large spatial scale without the complexities of *in-situ* modelling. For example, Yang et al., (2021) utilised the commercial CFD software ANSYS Fluent in order to determine the effectiveness of a submerged tidal current turbine (TCT) for scour mitigation and extra green energy production. CFD enabled the identification of a need for the correct positioning of the TCT at the base of the monopile for optimum performance. When used in conjunction with real-world measurements, its effectiveness can be increased even further through verification and validation.

The ability to accurately predict and quantify areas of high shear stress potentially occurring around structures using real-world conditions such as flow velocity, turbulence, and sediment type, can help inform the planning of installations with regard to location, engineering and design. When these conditions are taken into consideration, mitigation methods could be better adapted to suit the specific area identified at an early stage in the development process. However, these models require some degree of validation to verify outputs. Shipwrecks offer novel *in-situ* features with which to test theories of hydrodynamics and sediment transport around seabed objects, with CFD modelling offering a robust tool to do so. The aim of this paper is to develop a CFD model at a shipwreck site in order to simulate current flow patterns and magnitudes with which to better understand seabed morphological patterns of sediment erosion and deposition caused by the wreck's obstruction. When combined with other high-resolution seabed survey data, these outputs and understandings could potentially be applied to other critical offshore engineering as part of a robust methodology to assess the impacts of sediment dynamics and prevent scour and other adverse impacts.

2. Description of the Site

The *SS Polwell* is located approximately 10 km off the east coast of Ireland, north of Dublin, in the Irish Sea (Figure 1). It originally measured 86.56 x 11.6 x 5.53 metres and operated as a defensively-armed steam collier. It was torpedoed by a German submarine on 5th June 1918 with no loss of life. The wreck lies in approximately 30 m water depth, orientated NE-SW with the bow to the NE, on seabed comprising a multimodal distribution of sediment types (Majcher et al., 2021). Ground-truthing grab samples taken from the site suggest muddy sand and slightly gravelly muddy sand. To the south of the *SS Polwell* are a number of seabed ridges believed to be out-cropping bedrock or glacial till. Approximately 600 m to the north of the *SS Polwell* site a gas interconnector pipeline transverses east-west. Previous residual relief modelling highlighted extensive erosional and depositional features to the north of the site, with limited development to the south due to the presence of the seabed ridges (Majcher et al., 2020). Modelled data for seabed currents in the area suggest a dominant NW-SE direction of flow reaching a maximum of 0.4 m/s.

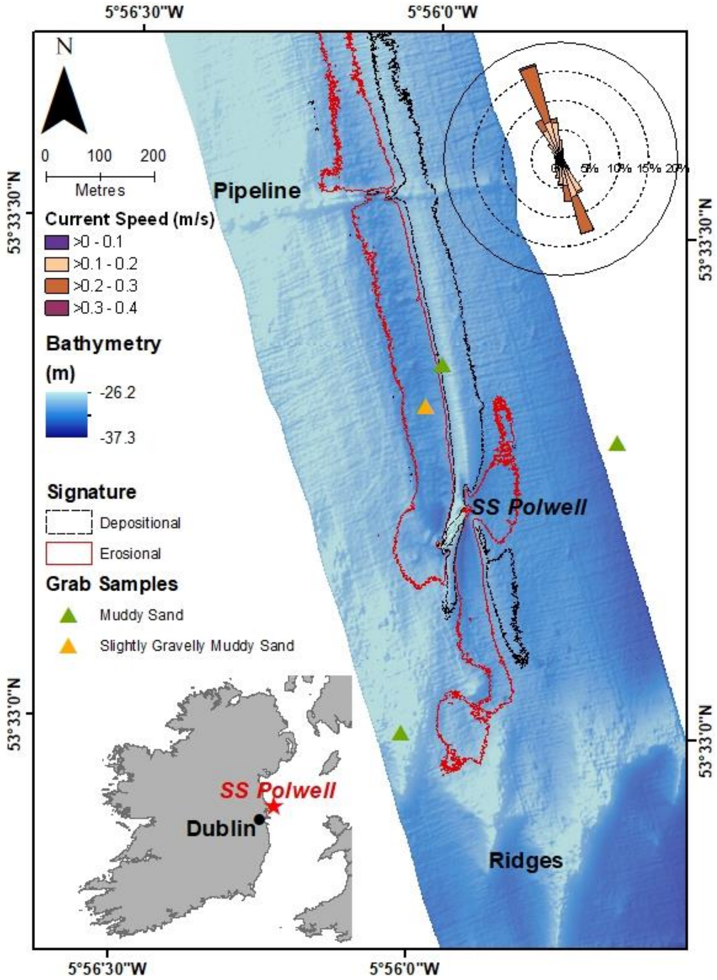

Figure 1. Location of the SS Polwell in the Irish Sea and site characterisation. Rose chart (top right) represents modelled data for near-seabed currents. Bathymetry data is presented with a hillshade effect (azimuth 315°, elevation 45°). Seabed signatures are delineated according to the approach of Majcher et al. (2020). Grab sample locations are represented by coloured triangles

This shipwreck has already been investigated as part of other studies (Westley et al., 2019; Majcher et al., 2021). Repeated high-resolution bathymetric data has been collected at the *SS Polwell* site onboard the *RV Celtic Voyager* as part of three separate surveys in 2015 (CV15021), 2016 (CV16031) and 2019 (CV19027) under the Marine Institute Ship-Time Programme, allowing for detailed and general site characterisation. In this study, bathymetric data collected as part of the CV19027 survey was used. The multibeam echosounder (MBES) data were acquired using a dual-head, hull-mounted Kongsberg EM2040 operating at 400 kHz, with a continuous wave pulse. An integrated GNSS/L-Band receiver CNAV 3050 provided primary position corrections, and a Seatex Seapath 330+ acted as a secondary positioning system as well as providing motion referencing and timing. Survey lines were aligned in a grid, which allowed for 110°- 120° swath coverage. Data from the 2019 survey were cleaned and processed in Caris HIPS and SIPS v. 9 using the the Combined Uncertainty and Bathymetry Estimator algorithm (CUBE; Calder & Wells, 2006), and were tidally corrected before being exported as digital elevation models (DEMs) as raster format in the UTM 30N projection. The horizontal resolution of this dataset is 0.2 m. More details on all data processing and compliance with IHO Special Order standards can be found in Majcher et al. (2020; 2021). DEM rasters were used as geometry input for CFD modeling efforts.

3. CFD Model

3.1 Computational Domain

Best practice guidance on domain size by Franke et al. (2007) suggests the domain should be based on the height and lateral extension of the obstacle involved. Mo et al. (2021) further expand on this for the flow of wind turbines. Although the subjects of these studies differ from the model included in this paper in that they are concerned with the flow of air as opposed to sea water, the overarching point remains valid: the domain size is relative to the dimensions of the object of the study. The cuboidal computational domain in this study represents a length of 100m, a width of 100m and a depth of 35m. The actual domain descends a further 10m vertically from the 3D geometry, which is situated at 0m, giving a Y axis value of -10m to +25m. This was required as the natural undulations on the seabed caused it to dip below 0m, exposing the base of the mesh and introducing interference into the model. Although Franke et al. (2007) suggests vertical extension at five times the height of the object, our model is limited by the depth of the wreck. The *SS Polwell* lies at a depth of 29.8m however, the surface of the sea is a dynamic and changing environment. The 4.8m excluded from the natural domain provides a buffer where tidal and wave induced influences might occur. At much greater depths the main concern would have been balancing computational power required with an adequate vertical study zone allowing full evolution of the flow. Mo et al. (2021) concluded that a computational domain size that is not large enough limits the full development of the flow.

This paper aimed to examine scour induced by flow around the wreck by highlighting zones of high shear stress. In this study, the area of seabed immediately adjacent to the shipwreck site of the *SS Polwell* was considered due to the fine-scale construction of the simulation domain and constraints on computing capacity in terms of runtime. The two areas most vital to this study were the approach flow and the wake of the *SS Polwell*. Therefore, the extension of the seabed provided by the bathymetric data was deemed adequate for the model.

3.2 Geometry

The geometry of the seabed and wreck of the SS Polwell were contained within a point cloud .asc file, with both being part of a singular datafile, as opposed to separate samples. This data was gathered as part of the 2019 (CV19027) Marine Institute Ship-Time Programme Survey, at a resolution of 0.5m. This file was then converted into a stereolithography (.stl) file to provide a 3 dimensional representation, as well as compatibility with OpenFOAM v_2012. In order to accurately represent the correct flow direction, the .stl file was processed in Blender version 2.92.0 and rotated to align with the dominant north-westerly flow. This was repeated for the south-easterly current direction to provide an accurate representation of flow in a diurnal system. The geometry was placed at point 0 on the z axis of the domain, 10m above the base of the mesh to avoid interference where the dips in the seabed would cross outside the computational domain. The seabed and wreck geometry were prescribed a predefined roughness length (Z_0) of 0.06m, representing rippled sand, as used by Quinn and Smyth (2017).

3.3 Computational Mesh

The computational mesh used in the simulations was created using OpenFOAM utilities *snappyHexMesh* and *blockMesh* (Figure 2). It is a hybrid mesh containing a structured background grid and an unstructured hexahedron-dominated mesh in the near-wall region. Each *blockMesh* cell was assigned a uniform size of 2m x 1m x 2m in all directions, with the geometry positioned at 0m on the Y axis. *SnappyHexMesh* was used to generate, position and refine the seabed and shipwreck geometry. The resulting mesh consisted of 264093 cells with 3 layers defined and an expansion ratio of 1.4. A mesh sensitivity study was performed, using coarser and finer meshes until mesh independence was achieved. The mesh was considered adequate when computational time was reduced to its minimum, while maintaining a suitable level of detail.

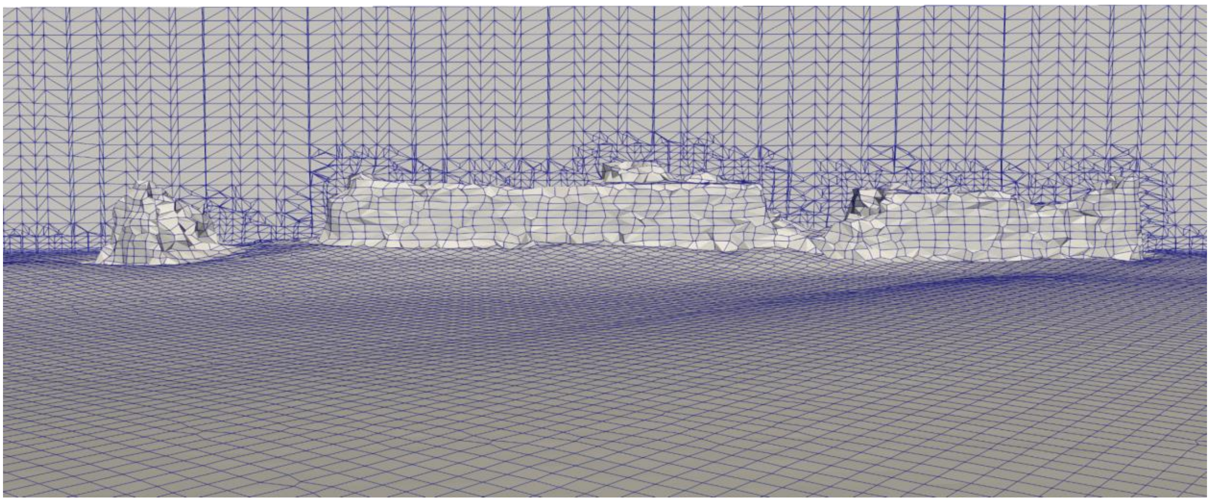

Figure 2. *Computational mesh including boundary cells and 3D geometry mesh*

3.4 Governing Equations

In the presented CFD model, the flow within the testing domain is assumed to be incompressible, Newtonian, and statistically steady, with temperature and gravity effects neglected. the flow is governed by the Reynolds-Averaged Navier-Stokes (RANS) formulation for mass and momentum:

$$\nabla\cdot\mathbf{U}=0$$

$$\nabla\cdot(\mathbf{UU})=\nabla\cdot[\nu_{eff}\,(\nabla\mathbf{U}+(\nabla\mathbf{U})^T)]-\nabla p \qquad (1)$$

where **U** is the time-averaged velocity, p is the time-averaged kinematic pressure (pressure divided by density), ν_{eff} is the effective kinematic viscosity which is the summation of laminar kinematic viscosity (ν) and the turbulent kinematic viscosity (ν_t). The value of ν is 1.307×10^{-6} m^2/s, representing water at (10 °C). The unknown ν_t is calculated from the turbulence kinetic energy (k) and the energy dissipation frequency (ω) using the k-ω SST (shear stress transport) turbulence model due to its ability to solve, in detail, at both the boundaries and the internal field.

In this study, the RANS simulations employ the SIMPLE algorithm to perform the pressure-velocity coupling (simpleFOAM solver in OpenFOAM-v2012). It is the steady state solver for incompressive, turbulent flow.

3.5 Boundary Conditions

The boundary domain (Figure 3) consisted of six faces, with fluid flow moving from the inlet to the outlet. Inlet and outlet boundary conditions were created at opposite sides to define a flow direction, with the geometry oriented to represent the prevailing current. The patch types assigned to each of the six faces are shown in Table 1.

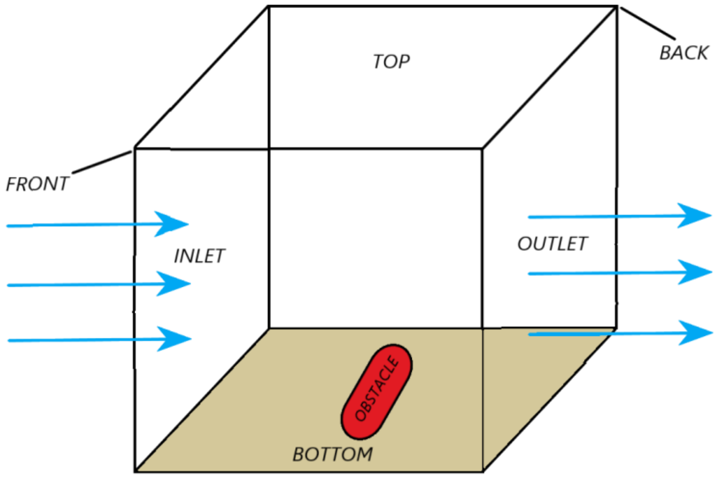

Figure 3. CFD model setup showing boundary types. Brown represents seabed, blue arrows represent flow direction

Table 1. *Setup of patch types for boundaries in blockmesh*

BLOCKMESH BOUNDARY FACE	***PATCH TYPE***
INLET	*PATCH*
OUTLET	*PATCH*
TOP	*SLIP*
BOTTOM	*WALL*
FRONT/BACK	*SYMMETRYPLANE*

A power-law velocity profile was generated at the inlet for U by using the equation described in Soulsby (1997) and Lewis et al. (2017):

$$\boldsymbol{Uz} = \left(\frac{z}{\beta\, h}\right)^{\frac{1}{\alpha}} \bar{U} \qquad (2)$$

Where the velocity profile (the velocity at height $\boldsymbol{Z}$ above the seabed **U***z*) is described using a power law ($\boldsymbol{\alpha}$) and bed roughness coefficient ($\boldsymbol{\beta}$), with water depth ($\mathbf{h}$) and depth averaged velocity (**Ū,** 0.147m/s at 1m from the seabed)**.** Current data for the *SS Polwell* was obtained from the Marine Institute of Ireland using output from their operational hydrodynamic model (Nagy et al., 2020), which is run on the Regional Ocean Modeling System (ROMS: Shchepetkin and McWilliams, 2005). Data was obtained for depth-averaged current velocity and direction for a 1-year period and used in site characterisation (see current speed rose Figure 1) and as inlet current speed values in CFD modelling efforts. Values were generated using the above formula and entered into a .csv file for use with the OpenFOAM *fixedProfile* boundary condition.

A summary of the boundary conditions of the five primary unknowns (U, p, k and ω and nut) applied at each boundary region is shown in Table 2.

Table 2. *Boundary conditions of simulations based on the k-ω SST model*

	P	**U**	**K**	**ω**	**NUT**
DIMENSIONS	*[0 2 -2 0 0 0 0]*	*[0 1 -1 0 0 0 0]*	*[0 2 -2 0 0 0 0]*	*[0 0 -1 0 0 0 0]*	*[0 2 -1 0 0 0 0]*
UNITS	*m^2/s^2*	*m/s*	*m^2/s^2*	*s^{-1}*	*m^2/s^{-1}*
INTERNALFIELD	*UNIFORM 0*	*UNIFORM (0 0 0)*	*UNIFORM 0.000013*	*UNIFORM 0.--206*	*UNIFORM 0*
INLET	*ZEROGRADIENT*	*FIXEDPROFILE*	*FIXEDVALUE; VALUE $INTERNALFIELD*	*FIXEDVALUE; VALUE UNIFORM 1*	*CALCULATED; VALUE UNIFORM 0*
OUTLET	*FIXEDVALUE; VALUE UNIFORM 0*	*ZEROGRADIENT*	*INLETOUTLET; INLETVALUE $INTERNALFIELD; VALUE $INTERNALFIELD*	*INLETOUTLET; INLETVALUE $INTERNALFIELD; VALUE $INTERNALFIELD*	*ZEROGRADIENT;*
TOP	*SLIP*	*SLIP*	*SLIP*	*SLIP*	*SLIP*
BOTTOM	*ZEROGRADIENT*	*ZEROGRADIENT*	*KQRWALLFUNCTION; VALUE $INTERNALFIELD*	*ZEROGRADIENT*	*NUTKWALLFUNCTION; VALUE UNIFORM 0*
FRONT/BACK	*SYMMETRYPLANE*	*SYMMETRYPLANE*	*SYMMETRYPLANE*	*SYMMETRYPLANE*	*SYMMETRYPLANE*
POLWELL	*ZEROGRADIENT*	*NOSLIP*	*KQRWALLFUNCTION; VALUE $INTERNALFIELD*	*OMEGAWALLFUNCTION; VALUE $INTERNALFIELD*	*NUTKWALLFUNCTION; Ks UNIFORM 0.000755; Cs UNIFORM 0.5; VALUE UNIFORM 0*

4. Results

CFD model outputs for flow velocity, flow patterns and bed shear stress were visualised and analysed in ArcMap version 10.7 and Paraview version 5.9.0. Analysis was carried out on results from two separate simulations representing the dominant flow directions: from NW to SE and SE to NW.

4.1 Flow Velocity and Patterns

Bed flow velocity values were derived from the cells immediately adjacent to the seabed. Figure 4 shows a maximum velocity value of 0.26m/s and a minimum value of 0.001m/s for the NW to SE flow and a maximum of 0.25m/s and a minimum of 0.006 for the SE flow. The mean current speed for the NE was 0.09m/s, and 0.08m/s for the SE.

Flow rates from the NW were divided and categorized as low velocity (0.001-0.07m/s), medium velocity (0.07-0.12m/s) and high velocity (>0.12m/s), based on the Jenks natural breaks classification of the velocity distribution. The Jenks natural breaks classification method determines the best arrangement of values into different classes by minimizing each class's average deviation from the mean, while maximizing each class's deviation from the means of the other groups (Chen et al., 2013). Flow rates for the SE were categorised as low velocity (0.0006-0.06m/s), medium velocity (0.06-0.11m/s), and high velocity (>0.11m/s).

Flow from the NW displays a large area of high velocity flow, directly in the central wake of the wreck (Figure 4a). This area is surrounded on either side by a low velocity area, wrapping itself around the wreck's bow and stern, producing a typical wake flow. The flow from the bow appears much more pronounced, flowing through the large break in the hull. Another small area of high velocity flow emerges on the outside of the bow wake, sandwiching the lower velocity flow in between itself and the central wake. As the approach fow makes contact with the wreck on its starboard side it produces two distinct areas of low velocity; at the stern and at the break in the midsection. The areas of high and low velocity are paralleled by a mid velocity flow on either side.

The high velocities in the flow from the SE to NW are concentrated mainly towards the bow of the wreck, pushing through the gap in the bow. The high velocity wake is intersected by a thin stream of low velocity flow and bordered by another to the SW. A large low velocity wake emerges from the stern, separated from the main high velocity wake by a low-mid flow. Again, the approach flow produces areas of low velocity upon reaching the wreck directly, however they span the entirety of the wreck from bow to stern, with a small high velocity area appearing in front of the separated bow section. A medium velocity flow runs either side of the main wake.

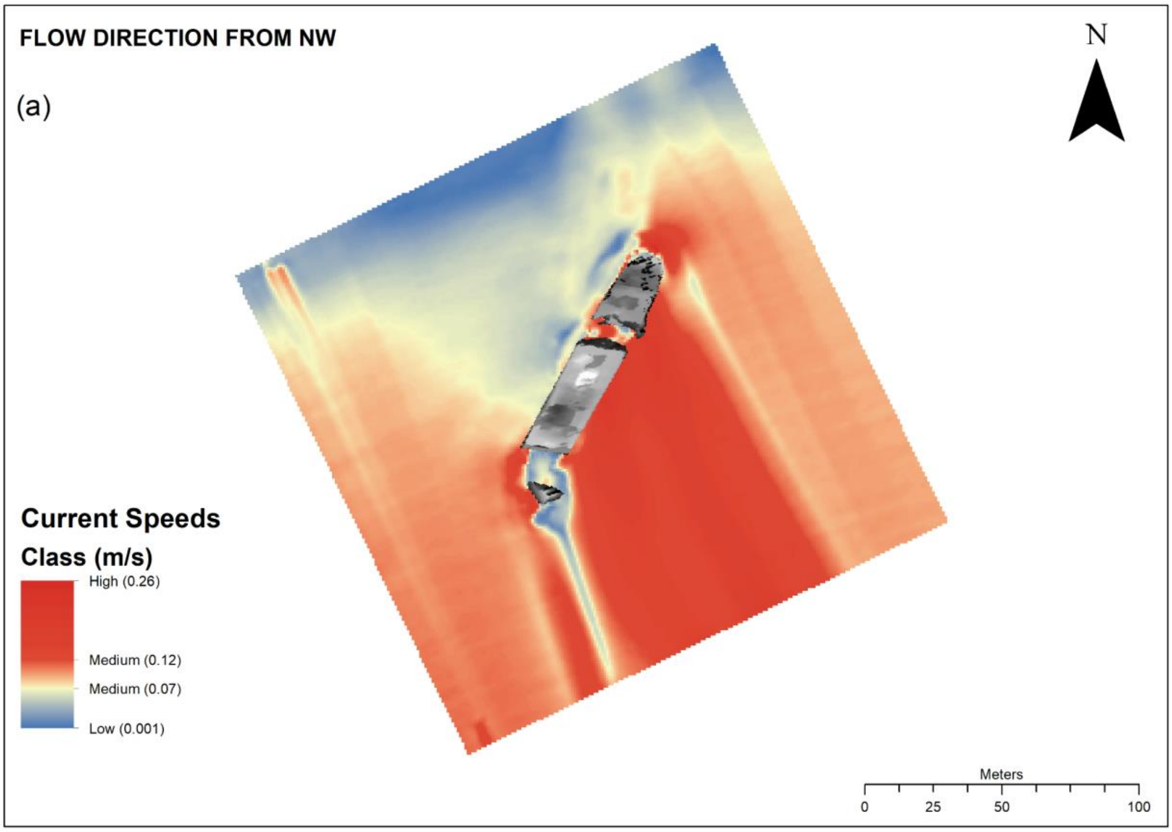

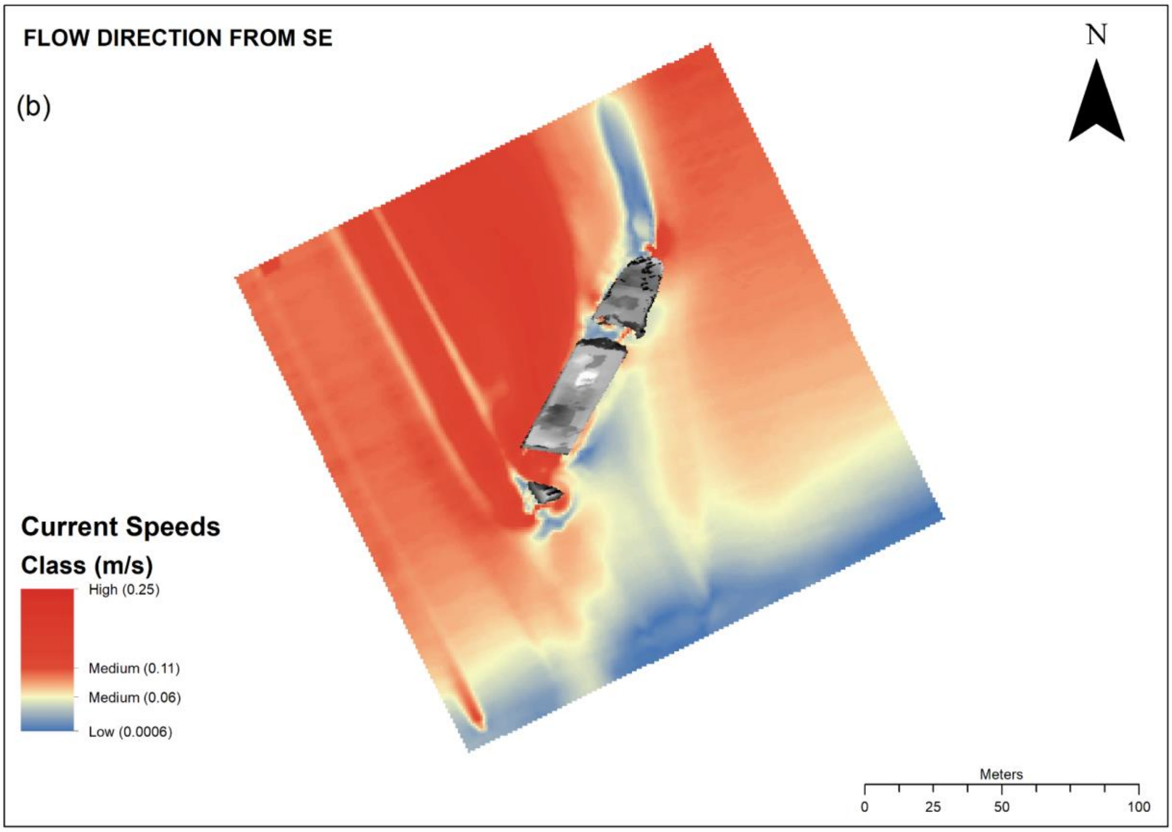

Figure 4. *Maps representing current velocities close to the seabed for flow from the NW (a) and flow from the SE (b)*

Streamline models were generated in ParaView for both current directions (Figures 5 & 6), showing more complex flow velocity patterns overlaid on bed shear stress values. Flow velocity for both directions ranged from 0.0047m/s to 0.22m/s.

Figure 5 shows the flow from the NW to SE. Laminar flow is dominant either side of the bow and stern of the wreck, where shear stress is minimal. As the flow interacts directly with the wreck however, complex patterns emerge in the wake where horizontal flow separation occurs. As water flows around the wreck's stern, it turns inward towards the wreck where two major low velocity vortices form. These vortices occur where the bed shear stress is highest, losing rotation as they continue towards the outflow of the study area. The break towards the ship's stern appears to be a major contributing factor towards the formation of these vortices.

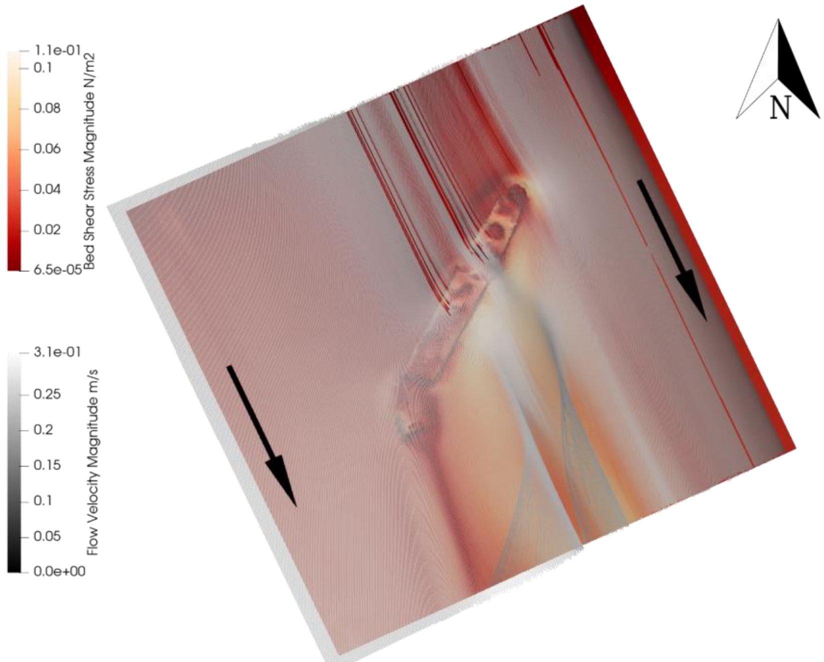

Figure 5. *Streamlines representing current velocity in flow from NW to SE*

The SE to NW flow shows a similar pattern of vortices where it interacts with the wreck, with steady, laminar flows either side (Figure 6). Similarly it shows the formation of two distinct vortices, through the gap in the hull towards the bow of the ship; the first, towards the east is a significantly developed, low velocity vortex stretching all the way to the stern before being contained by the surrounding flow; the second, towards the west, is a far less developed vortex, distinguished from the surrounding flow by its lower velocity and slight rotation. Again, where both vortices occur bed shear stress is at its highest.

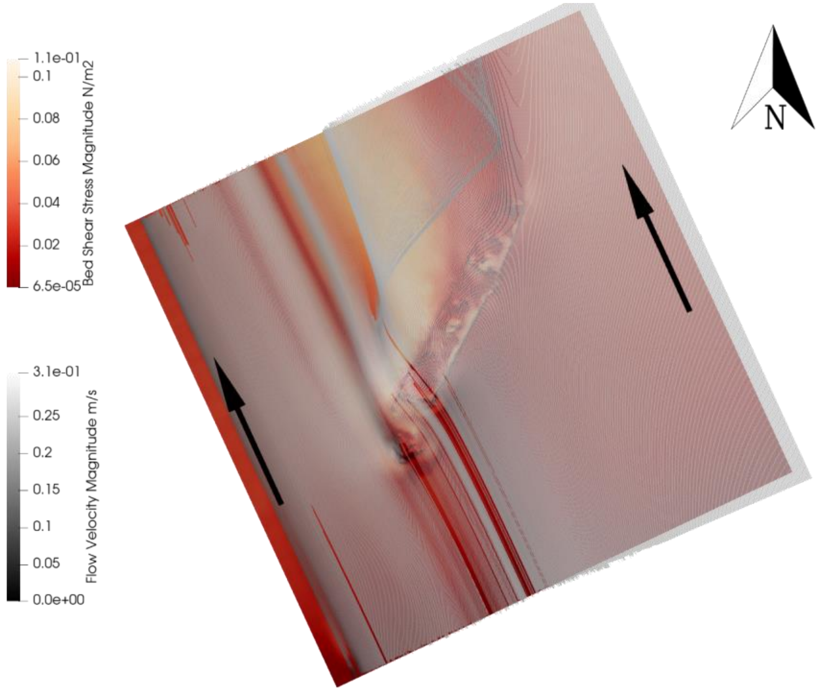

Figure 6. *Streamlines representing current velocity in flow from SE to NW*

4.2 Bed Shear Stress

In sediment mobility studies, current speeds are converted to bed shear shear stress to assess the force acting on a particular sediment type (e.g. Whitehouse, 1998). In OpenFOAM, the bed (or wall) shear stress vector (τ_c) is calculated using the built-in *wallShearStress* function at selected wall patches using the equation $\tau c = R \cdot n$, where R is shear-stress symmetric tensor retrieved from the turbulence model and n is the patch normal vector (into the domain). The resulting values were given in m^2/s^2. By using the calculator function within Paraview, we multiplied our wall shear stress values by our fluid density (seawater at 10 °C, 1027 kg/m^3) in order to give values in Pascals. Figure 7 shows bed shear stress overlaid with areas exhibiting erosional and depositional signatures defined from survey data by Majcher et al. (2021). The flow originating from the NW displays a maximum value of 0.091Pa and a minimum of 0.00008Pa, with a mean of 0.03Pa (Figure 7a). Flow from the SE displays a maximum value of 0.085Pa and a minimum of 0.00008Pa, with a mean of 0.026Pa (Figure 7b). Both flow directions were also characterized separately as having areas of high, medium, and low shear stress based on natural breaks in the data distribution. Flow rates for the NW were categorised as low shear stress (0.00008-0.02Pa), medium shear stress (0.02-0.04Pa), and high shear stress (>0.04Pa). Flow rates for the SE were categorised as low shear stress (0.00008-0.02Pa), medium shear stress (0.02-0.05Pa), and high shear stress (>0.05Pa).

Flow from the NW displays a large area of high shear stress in the centre of the wreck's wake, surrounded on either side by areas of low stress. Another, thin area of high stress wraps around the highly defined low stress emerging from the wake of the wreck's bow. There is a small area of high stress in the midship break and a prominent one at the point of the wreck's stern. A large area of low stress is present in the approach flow, making contact with the full length of the wreck. Areas of medium stress are present on either side of the wake.

Flow from the SE displays a large area of high stress in the wreck's wake, skewed towards the bow. Two thin lines of low stress emerge on the SW side of the high stress; one intersecting an area of medium-high stress; the other bordering it. A large, well defined area of low stress emerges from the stern wake, with a very small area of high stress at the point of the stern and a slightly larger one in the gap between the bow and the main section. As with the NE flow, the approach flow contains a large, low stress area that makes contact along the length of the wreck.

The seabed signature patterns of erosional and depositional areas suggest a symmetry, with significant erosional areas adjacent to the wreck on the west side and the east side. A separate large area of deposition occurs to the SE, with a thin signature of low deposition slightly north. Neither of these areas show a symmetrical comparison to the NW. The areas of erosion and deposition represented by the previous survey data compare well with the areas of high and low shear stress generated from the model outputs. In the wreck's wake the boundaries outlining erosional effects follow the model predictions closely, with high shear stress in the centre. The areas outside this high stress area, where velocity and shear stress drop to low values, are outlined by areas of deposition from the survey data. The *SS Polwell* itself is located in a signature indicating an area of deposition, with the model outputs showing low shear stress in the vicinity of the wreck body.

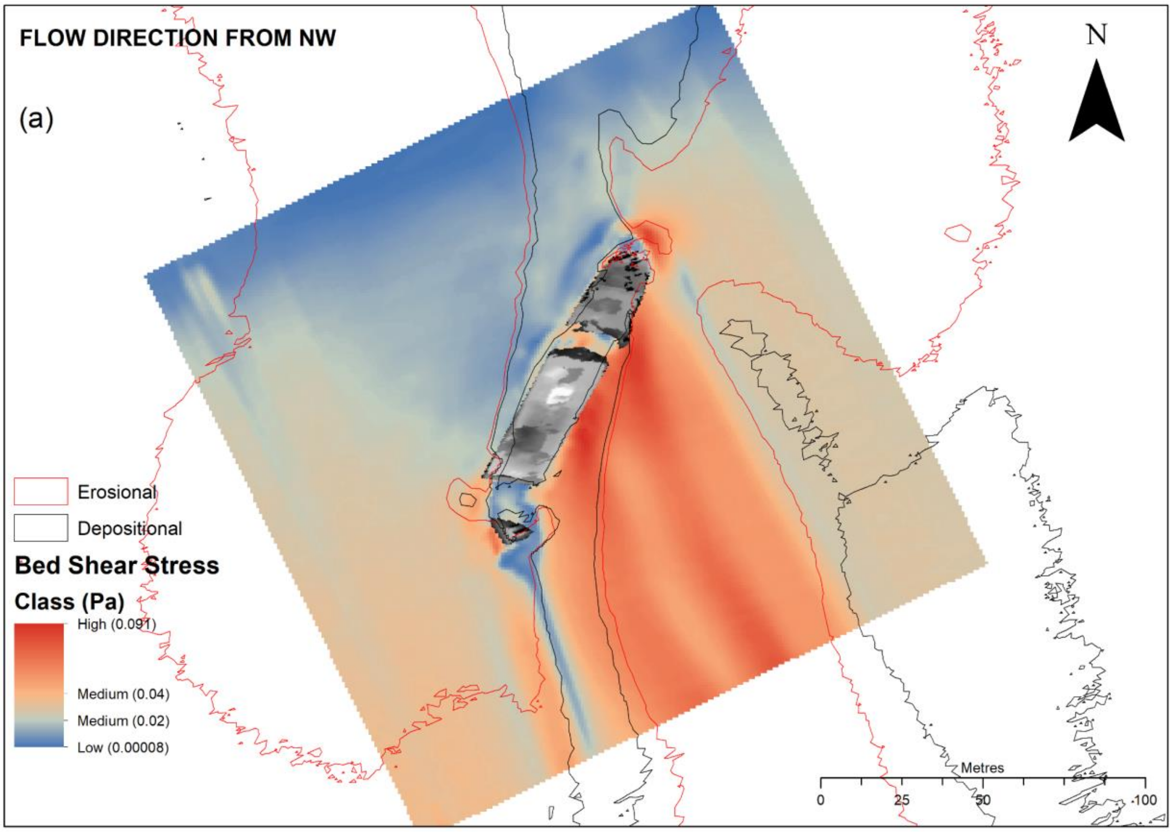

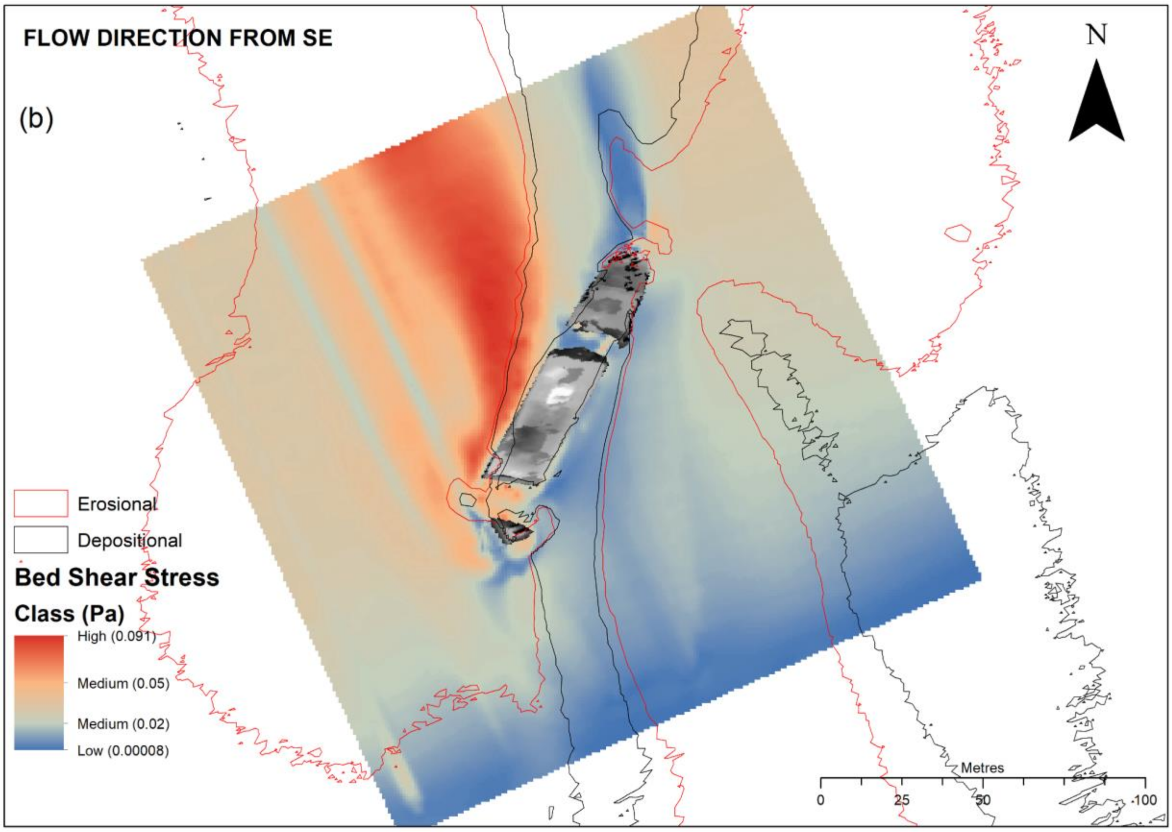

Figure 7. *Maps representing bed shear stress with flow from the NW (a) and flow from the SE (b). Red and black lines represent areas of erosion and deposition*

5. Discussion

5.1 CFD Model Simulations and Validity

The results from this study suggest that, despite a complex interaction of hydrodynamics with a seabed obstacle (i.e. a shipwreck), CFD modeling is capable of producing outputs that can be validated using real-world survey data to explain seabed sediment dynamics. Previous studies have sought to understand seabed hydrodynamics and scour through the sole use of repeat surveys or *in-situ* monitoring devices, or a combination of both (Bauri and Sarkar 2016; Majcher et al., 2020). By examining a summation of survey data, velocity values, shear stress, and flow regimes we have created a multidimensional, multipurpose model.

Examination of the current velocity shows a typical flow pattern in the wreck's wake where pressure gradients created by flow around and over the wreck result in increased velocity in the centre of the wake, with less energetic flows on either side. (Quinn and Smyth, 2018). The median values of 0.1305m/s for the NW flow, and 0.1253m/s for the SE flow, reflect the slightly higher current velocities from the NW. Velocity values in the immediate vicinity of the wreck, excluding the wake areas, show an amplification of velocity when compared to the mean depth averaged velocity of 0.147m/s. Flow from the NW to SE shows an amplification factor of 2, as does flow from the SE to NW. This broadly agrees with findings from Smyth and Quinn (2014) and Whitehouse (1998), where they highlight that flow is amplified by the presence of a wreck or obstacle, including the immediate wake, by a factor of 3 to 4: an order higher than those presented here.

The patterns of velocity correspond well to the patterns of shear stress, creating near mirror images. The patterns of shear stress suggest an area of erosion in the centre of the wreck's wake, with deposition on either side and where the approach flow contacts the wreck itself. This is supported by the previous survey data overlaid, showing areas of erosion and deposition by examining changes in depth. These patterns of velocity and shear stress correlate well with the overlaid survey data in that where high shear stress occurs erosion takes place, and where low shear stress occurs, deposition takes place. This serves to provide effective validation of the model.

It is known however, from temporal comparison of repeat survey data that the *SS Polwell* and the area adjacent do not show any signs of significant scour, typically -0.02 to -0.04 m on an interannual basis, instead suggesting a slight tendency towards deposition (Majcher et al., 2020). This is probably due to a combination of factors, rather than a single overall influence. Current speed in the area is considered to be relatively low in the area when compared to other shipwreck sites examined by Majcher et al. (2021) (e.g. *SS Hare*, *SS Tiberia*). With less energetic currents in the area on average throughout the year, combined with too great a depth for the wave base to interact with the seabed, the mobilisation of sediment is less likely to occur. Additionally, the presence of diurnal tides of equal magnitude would work to, at least partially, negate the mass transport of sediment outside the immediate area. The *SS Polwell* lies in a multimodal sediment, composed of gravelly muddy sand, with muddy sand further out (Figure. 1). This could have contributed to the lack of scour in that the finer mud has already been transported, or winnowed, from the area, leaving the coarser grains behind as a lag. This gravelly, muddy sand would require a higher threshold of mobilisation when compared to finer mud or sand.

When examined closely, the flow patterns of the streamline models produced in OpenFOAM show that the vortices produced in the high areas of shear stress in the wreck's wake, are actually lower in velocity than the current close to the seabed. This suggests that rather than working to transport suspended sediment out of the system, the vortices enable suspension of the sediment in place. The higher velocities may exceed the mobilisation threshold, lifting the sediment into the vortex where the lower velocity cause it to dip back below the threshold, effectively resettling sediment back into to the seabed where it is lifted from again, creating a cycle until slack water signals reversal of the flow and temporarily interrupts the cycle.

5.2 Limitations and Recommended Further Work

The domain size of the study area sampled may not be sufficiently large to fully resolve the dynamic nature of the regional area. The inlet approach in particular may not allow for full development of the flow before reaching the *SS Polwell.* For example, to the north of the wreck site lies a pipeline in a roughly west to east orientation, and to the south lies an area of complex bedforms, both of which may further complicate the flow regime by introducing further obstructions to perturb tidal currents (Figure 1). The high-resolution nature of the input bathymetry data meant that CFD simulations for a larger area incorporating these features would require too much computer processing power in the context of this study. In order to better constrain inlet conditions for the high-resolution model domain of the immediate wreck site and generate more realistic flow simulations, a coarser-resolution model could be developed initially for a larger domain area in the up- and down-stream directions of tidal current flow. This model would capture regional flow patterns and the outputs could be used as input along the boundary of the smaller, high-resolution model.

For the purposes of this study the steady-state solver SimpleFOAM was employed as this study was focused specifically on verification and validation of a CFD model using data taken from a single survey (4th-10th October 2019). However, seabed sediment dynamics, and in particular scour development, can evolve significantly over time and so require transient solvers (Quinn and Smyth, 2018; Smyth and Quinn, 2014). At the *SS Polwell* site there is repeat bathymetric survey data that would allow for assessment of geomorphic change over varying temporal time-scales ranging from 1-week to 1-year to 4-years. Detailed analysis of these temporal changes would require a large-scale transient solver such as PimpleFOAM in order to provide an in-depth analysis of scour evolution over time.

The multimodal nature of sediment at the seafloor of the *SS Polwe*ll site represents a complex geological setting in terms of sediment distribution (Figure 1). As a result, no single value for the threshold of movement can be applied to the site to determine sediment mobility, making it difficult to calculate net movement of sediment and precise levels of scour or deposition. The mobilisation of the sediment particles is governed by the Shields parameter:

$$\boldsymbol{\tau}^* = \boldsymbol{\tau}/(p\text{s} - p)\text{gD}'$$

where:

- $\boldsymbol{\tau}$ is the dimensional shear stress;
- *p*s is sediment density;
- *p* is the fluid density;
- g is the gravitational acceleration;
- D is the particle diameter of the sediment.

Pang et al. (2016) demonstrated a critical Shields value that corresponds with the equilibrium scour depth. Previously, Majcher et al. (2021) utilised regionally modelled current speed data from the Marine Institute ROMS-based model to calculate exceedance values for sediment types at differing shipwreck sites. As highlighted in this study, values for current speed across a site with an obstacle (i.e. a shipwreck) can vary considerably depending on amplification factors associated with that obstacle, as well as seabed morphology. In this instance, current velocities were increased two-fold in the immediate vicinity of the wreck. Using more detailed current speed and calculated bed-stress data outputs from the model developed in this study, in conjunction with a sediment grain-size database, would allow for a much more robust assessment of sediment mobility due to threshold exceedance.

The Integrated Mapping for the Sustainable Development of Ireland's Marine Resource (INFOMAR) programme has been mapping the Irish seabed since 2006, and in that time has mapped some 457 shipwrecks in varying degrees of detail. The quality of this database, and it's broad geographic extent, means that the approach described here can be applied to a significant number of other sites in the Irish territory in differing hydrodynamic and seabed morphological and sedimentary settings. A future examination of multiple seabed obstructions and/or morphology types and their effects on the overall flow regime in this manner could serve to elucidate the complex nature of obstacle induced hydrodynamic flow and scour development, allowing for an extensive, regional assessment of scour potential.

6. Conclusion

Our study takes a novel approach, creating high-resolution models from bathymetric survey data to use as inputs in CFD simulations in OpenFOAM software. In turn, these simulations can be used to study the complex interaction between seafloor hydrodynamics and seabed objects. Modelled outputs for current flow and stress patterns correspond well with known seabed signatures for sediment erosion and deposition from survey data. The outputs from this approach can also be used in conjunction with repeat and physical (i.e. grab sample) survey data in order to understand temporal sediment dynamics and morphological change at a localised level. Ultimately this approach can be adapted and applied to other man-made structures (such as offshore wind turbine foundation structures) on the seabed as part of engineering design studies to mitigate against the risk of scour causing instability.

Acknowledgments

This project is funded by the Geological Survey of Ireland (GSI) Geoscience Research Programme under their 2020 Short Calls. Acquisition of bathymetry data was supported by the Marine Institute of Ireland's ship-time programme's APP-CV15021, CV16031: *World War I shipwrecks in the Irish Sea: commemoration, visualization and heritage management* and APP-CV19027: *Geohazard investigation in the Irish Sea using seismic and seabed mapping techniques (GIST)*. The authors thank the crew of the *RV Celtic Voyager* on these surveys for their skill and dedication, as well as Rory Quinn, Ruth Plets, Chris McGonigle, Kieran Westley and Fabio Sacchetti for provision of data and support. The authors also express their gratitude to the MI Oceanographic Services Team for their support with ocean current data requests. JM is supported by an Ulster University Vice-Chancellor's Research Studentship. MC is funded under an Irish Research Council Enterprise Partnership Scheme Postdoctoral Fellowship (EPSPD/2020/109) and in part by a research grant from Science Foundation Ireland (SFI) under Grant Number 13/RC/2092, with support from Gavin and Doherty Geosolutions Ltd and the Geological Survey of Ireland (GSI).

References

Bauri, K.P. and Sarkar, A., 2016. Flow and scour around vertical submerged structures. *Sādhanā*, *41*(9), pp.1039-1053.

Calder, B. and Wells, D.E., 2007. CUBE user's manual. Durham: University of New Hampshire. http://ccom.unh.edu/sites/default/files/publications/Calder_07_CUBE_User_Manual.pdf

Chen, J., Yang, S., Li, H., Zhang, B. and Lv, J., 2013. Research on Geographical Environment Unit Division Based on the Method of Natural Breaks (Jenks). *The International Archives of the Photogrammetry, Remote Sensing and Spatial Information Sciences*, XL-4/W3, pp.47-50.

Fernández-Montblanc, T., Izquierdo, A., Quinn, R. and Bethencourt, M., 2018. Waves and wrecks: A computational fluid dynamic study in an underwater archaeological site. *Ocean Engineering*, 163, pp.232-250.

Franke, J., Hellsten, A., Schlunzen, K.H. and Carissimo, B., 2011. The COST 732 Best Practice Guideline for CFD simulation of flows in the urban environment: a summary. *International Journal of Environment and Pollution*, *44*(1-4), pp.419-427.

Li, Y., Ong, M.C., Fuhrman, D.R. and Larsen, B.E., 2020. Numerical investigation of wave-plus-current induced scour beneath two submarine pipelines in tandem. *Coastal Engineering*, *156*, p.103619.

Ma, H. and Chen, C., 2021. Scour protection assessment of monopile foundation design for offshore wind turbines. *Ocean Engineering*, *231*, p.109083.

Majcher, J., Plets, R. and Quinn, R., 2020. Residual relief modelling: Digital elevation enhancement for shipwreck site characterisation. *Archaeological and Anthropological Sciences*, *12*, pp.1-13.

Majcher, J., Quinn, R., Plets, R., Coughlan, M., McGonigle, C., Sacchetti, F. and Westley, K., 2021. Spatial and temporal variability in geomorphic change at tidally influenced shipwreck sites: The use of time-lapse multibeam data for the assessment of site formation processes. *Geoarchaeology*, *36*(3), pp.429-454.

Matutano, C., Negro, V., López-Gutiérrez, J.S. and Esteban, M.D., 2013. Scour prediction and scour protections in offshore wind farms. *Renewable energy*, *57*, pp.358-365.

Mellet, C., Long, D., Carter, G., Chiverrell, R., Van Landeghem, K., 2015. Geology of the seabed and shallow subsurface: The Irish Sea. *British Geological Survey Commissioned Report, CR/15/057.* 52pp.

Mo, J.O., Choudhry, A., Arjomandi, M., Kelso, R. and Lee, Y.H., 2013. Effects of wind speed changes on wake instability of a wind turbine in a virtual wind tunnel using large eddy simulation. *Journal of Wind Engineering and Industrial Aerodynamics*, *117*, pp.38-56.

Nagy, H., Lyons, K., Nolan, G., Cure, M., & Dabrowski, T. 2020. A Regional Operational Model for the North East Atlantic: Model Configuration and Validation. *Journal of Marine Science and Engineering,* Vol. 8, Issue 9. https://doi.org/10.3390/jmse8090673

Pang, A.L.J., Skote, M., Lim, S.Y., Gullman-Strand, J. and Morgan, N., 2016. A numerical approach for determining equilibrium scour depth around a mono-pile due to steady currents. *Applied Ocean Research*, *57*, pp.114-124.

Quinn, R., Bull, J. and Dix, J., 1997. Buried scour marks as indicators of palaeo-current direction at the Mary Rose wreck site. *Marine Geology*, 140(3-4), pp.405-413.

Quinn, R. and Smyth, T.A.G., 2018. Processes and patterns of flow, erosion, and deposition at shipwreck sites: a computational fluid dynamic simulation. *Archaeological and Anthropological Sciences*, *10*(6), pp.1429-1442.

Schendel, A., 2018. *Wave-current-induced scouring processes and protection by widely graded material* (Doctoral dissertation, Hannover: Institutionelles Repositorium der Leibniz Universität Hannover).

Shchepetkin, A.F. and McWilliams, J.C., 2005. The regional oceanic modeling system (ROMS): a split-explicit, free-surface, topography-following-coordinate oceanic model. *Ocean modelling*, *9*(4), pp.347-404.

Smyth, T. and Quinn, R., 2014. The role of computational fluid dynamics in understanding shipwreck site formation processes. *Journal of Archaeological Science*, 45, pp.220-225.

De Vos, L., De Rouck, J., Troch, P. and Frigaard, P., 2011. Empirical design of scour protections around monopile foundations: Part 1: Static approach. *Coastal Engineering*, *58*(6), pp.540-553.

De Vos, L., De Rouck, J., Troch, P. and Frigaard, P., 2012. Empirical design of scour protections around monopile foundations. Part 2: Dynamic approach. *Coastal Engineering*, *60*, pp.286-298.

Welzel, M., Schendel, A., Hildebrandt, A. and Schlurmann, T., 2019. Scour development around a jacket structure in combined waves and current conditions compared to monopile foundations. *Coastal Engineering*, *152*, p.103515.

Westley, K., Plets, R., Quinn, R., McGonigle, C., Sacchetti, F., Dale, M., McNeary, R., & Clements, A. 2019. Optimising protocols for high-definition imaging of historic shipwrecks using multibeam echosounder. *Archaeological and Anthropological Sciences*, 3629–3645. https://doi.org/10.1007/s12520-019-00831-6

Whitehouse, R., 1998. *Scour at marine structures*. London: Thomas Telford Ltd.

Whitehouse, R.J., Sutherland, J. and Harris, J.M., 2011, December. Evaluating scour at marine gravity foundations. In *Proceedings of the Institution of Civil Engineers-Maritime Engineering* (Vol. 164, No. 4, pp. 143-157). Thomas Telford Ltd.

Yang, B., Wei, K., Yang, W., Li, T. and Qin, B., 2021. A feasibility study of reducing scour around monopile foundation using a tidal current turbine. *Ocean Engineering*, *220*, p.108396.